

WL-TR-97-4130

**INTELLIGENT CONTROL AND OPTIMAL DESIGN
SYSTEM FOR METAL FORMING PROCESSES**



Harold L. Gegel, Ph.D.

UES, Inc.
4401 Dayton-Xenia Road
Dayton, OH 45432-1894

July 1997

19980324 092

Final Report For the Period 15 June 1995 - 14 June 1997

This is a Small Business Innovation Research (SBIR) Phase II Report.

Approved for Public Release; Distribution is Unlimited.

Materials Directorate
Wright Laboratory
Air Force Materiel Command
Wright-Patterson Air Force Base, Ohio 45433-7251

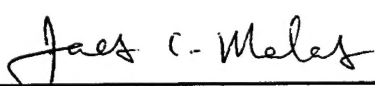
DTIC QUALITY INSPECTED 8

NOTICE


When Government drawings, specifications, or other data are used for any purpose other than in connection with a definitely related Government procurement operation, the United States Government thereby incurs no responsibility nor any obligation whatsoever; and the fact that the government may have formulated, furnished, or in any way supplied the said drawings, specifications, or other data, is not to be regarded by implication or otherwise as in any manner licensing the holder or any other person or corporation, or conveying any rights or permission to manufacture, use, or sell any patented invention that may in any way be related thereto.

This report has been reviewed by the Office of Public Affairs (ASC/PA) and is releasable to the National Technical Information Service (NTIS). At NTIS, it will be available to the general public, including foreign nations.

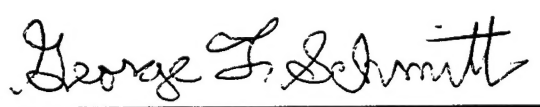
This technical report has been reviewed and is approved for publication.



DR. JAMES C. MALAS
Project Engineer
Material Process & Design Branch
Integration & Operations Division



DR. STEVEN LeCLAIR
Chief
Material Process & Design Branch
Integration & Operations Division



GEORGE SCHMITT
Chief
Integration & Operations Division
Materials Directorate

"If your address has changed, if you wish to be removed from our mailing list, or if the addressee is no longer employed by your organization please notify WL/MLIM, Bldg. 653, 2977 P St., Suite 13, W-PAFB, OH 45433-7251 to help us maintain a current mailing list."

Copies of this report should not be returned unless return is required by security considerations, contractual obligations, or notice on a specific document.

REPORT DOCUMENTATION PAGE

FORM APPROVED
OMB NO. 0704-0188

Public reporting burden for this collection of information is estimated to average 1 hour per response, including the time for reviewing instructions, searching existing data sources, gathering and maintaining the data needed, and completing and reviewing the collection of information. Send comments regarding this burden estimate or any other aspect of this collection of information, including suggestions for reducing this burden, to Washington Headquarters Services, Directorate for Information Operations and Reports, 1215 Jefferson Davis Highway, Suite 1204, Arlington, VA 22202-4302, and to the Office of Management and Budget, Paperwork Reduction Project (0704-0188), Washington, DC 20503.

1. AGENCY USE ONLY (Leave Blank)		2. REPORT DATE July 1997	3. REPORT TYPE AND DATES COVERED Final 06/15/95 - 06/14/97
4. TITLE AND SUBTITLE Intelligent Control and Optimal Design System for Metal Forming Processes		5. FUNDING NUMBERS C F33615-95-C-5822 PE 65502F, 62102F PR 3005 TA 05 WU B5	
6. AUTHOR(S) Harold L. Gegel, Ph.D.		8. PERFORMING ORGANIZATION REPORT NUMBER	
7. PERFORMING ORGANIZATION NAME(S) AND ADDRESS(ES) UES, Inc. 4401 Dayton-Xenia Road Dayton, OH 45432-1894		10. SPONSORING/MONITORING AGENCY REP NUMBER WL-TR-97-4130	
9. SPONSORING MONITORING AGENCY NAME(S) AND ADDRESS(ES) Wright Laboratory, Materials Directorate Air Force Materiel Command Wright-Patterson AFB, OH 45433-7251 POC: Dr. James C. Malas, WL/MLIM, Phone: (937) 255-8787			
11. SUPPLEMENTARY NOTES			
12a. DISTRIBUTION/AVAILABILITY STATEMENT Approved for Public Release; Distribution is Unlimited.		12b. DISTRIBUTION CODE	
13. ABSTRACT A new process design method for controlling microstructure development during hot metal deformation processes was developed. This approach is based on modern control theory and involves state-space models for describing the material behavior and the mechanics of the process. The challenge of effectively controlling the values and distribution of important microstructural features can now be systematically formulated and solved in terms of an optimal control problem. This method has been applied to the optimization of grain size and certain process parameters such as die geometry profile and applied to the optimization of grain size and certain process parameters such as die geometry profile and ram velocity during extrusion of plain carbon steel. Various case studies have been investigated, and experimental results show good agreement with those predicted in the design stage. A software product for <i>Microstructure Trajectory Optimization</i> was developed, and it is now ready for beta site testing. Modeling and simulation of metal forming equipment was done to better understand and improve the control of metal forming equipment. Techniques were developed for creating accurate models and computer simulations of metal forming equipment for the purpose of improving metal forming process design. Special emphasis was placed on modeling the dynamic behavior of hydraulic vertical forge presses, although similar principles apply to other types of metal forming equipment. Report developed under SBIR contract.			
14. SUBJECT TERMS SBIR Report Microstructure, Deformation, Forming.		15. NUMBER OF PAGES 124	
		16. PRICE CODE	
17. SECURITY CLASSIFICATION OF REPORT Unclassified	18. SECURITY CLASS OF THIS PAGE Unclassified	19. SECURITY CLASS OF ABSTRACT Unclassified	20. LIMITATION ABSTRACT SAR

TABLE OF CONTENTS

1.0	SUMMARY	1
2.0	INTRODUCTION	4
2.1	Program Objectives	6
2.2	Program Task	6
2.3	Program Deliverables	7
3.0	BACKGROUND	8
4.0	SOFTWARE DEVELOPMENT	11
4.1	Metallurgist Notepad	11
4.1.1	Requirements and Design	12
4.1.2	Usability	12
4.1.3	Processing Maps	13
4.1.4	Microstructures	14
4.1.5	Data Verification and Validation	14
4.1.6	Flow Curve Analysis and Adiabatic Temperature Correction	15
4.1.7	Data Import and Export	15
4.1.8	Material Processing Database	16
4.1.9	Software Architecture	16
4.1.10	Current Status	17
4.1.11	Future Development	19
4.2	Microstructure Optimization	21
4.2.1	Introduction	21
4.2.2	Description of Direct Extrusion	23
4.2.3	Microstructural Evolution During Hot Deformation	24
4.2.4	The Two-Stage Approach to Optimal Control of Deformation Processes	25
4.2.5	Material Behavior and Process Modeling Issues	27
4.2.6	Material Behavior Constraints and Optimality Criteria	28
4.2.7	General Formulation of the Optimal Control Problem	29
4.2.8	Optimality Criteria for Microstructure Development	30
4.2.9	Solution of the Microstructure Development Trajectory Optimization Problem	32
4.2.10	Application of the Two-Stage Optimization To Steel Extrusion ..	32
4.2.10.1	Models for Dynamic Recrystallization of Steel	32
4.2.10.2	First Stage: Formulation of a Cost Functional and Trajectory Optimization	36

4.2.10.3	Stage Two: Process Mechanics Control and Optimal Die Design	42
4.2.10.4	Comparison with Standard Die Designs	44
4.2.11	Summary and Conclusions	48
4.3	Modeling and Simulation of Metal Forming Equipment	49
4.3.1	Introduction	49
4.3.2	Press System Description	50
4.3.2.1	Hydraulics	51
4.3.2.1.1	Pumps	51
4.3.2.1.2	Head Pressure	52
4.3.2.1.3	Ram Pressure	53
4.3.2.1.4	Counter-balance Pressure	54
4.3.2.2	Servovalves	55
4.3.2.3	Ram Dynamics	57
4.3.2.4	Sensors	59
4.3.3	Computer Simulation of Dynamic Systems	61
4.3.3.1	Graphical Simulation Paradigm	62
4.3.3.2	Automatic Equipment Simulation Code Generation for the Metal Forming Industry	64
4.3.4	Application to the Drie 1000 ton Forge Press	65
4.3.5	Erie Press Simulation	66
4.3.6	Conclusions	71
4.4	Precision Die Design	72
4.4.1	Introduction	72
4.4.2	Forging Design Rules for Quality Assurance	74
4.4.2.1	Dimensional Control	74
4.4.2.2	Forging Envelope	75
4.4.2.3	Design to Achieve Mechanical Properties	82
4.4.3	Material Control	83
4.4.3.1	Work Flow Process for Die Design	90
4.4.3.2	Stress and Strain Concentration Factors	94
4.5	Shape Optimization	102
4.5.1	Introduction	102
4.5.2	Governing Equations for Material Flow	107
5.0	CONCLUSIONS	110
6.0	COMMERCIALIZATION	113
7.0	REFERENCES	114

LIST OF FIGURES

- Figure 1. View of MME Data, and Control of Data for Maps
- Figure 2. Dynamic Material Ti-6Al-4V Structurally Porous Material (SPM)
- Figure 3. Extrusion Process
- Figure 4. Schematic Representation of Dynamic Recrystallization
- Figure 5. Block Diagram of the Two-Stage Approach
- Figure 6. Penalty Function ($f(x,a,b)$) for Constraining Process Parameters Between a and b
- Figure 7. Strain-Rate Trajectories
- Figure 8. Temperature Trajectories
- Figure 9. Strain Trajectories
- Figure 10. Recrystallization Grain Size Trajectories
- Figure 11. Die Profiles
- Figure 12. Microstructures at Location of (first) Critical Strain and Die Exit
- Figure 13. Measured and Corrected Prior Austenite Grain Size Versus Position Along Die Centerline
- Figure 14. Simulated Temperature Distribution Along Die Centerline During Air Cooling Period
- Figure 15. Simplified Block Diagram of a Typical Hydraulic Press
- Figure 16. Typical Flow Curve for a Servovalve as a Function of Spool Position
- Figure 17. Vissim™ WINDOW, Top Level Diagram of a Forging Process Simulation
- Figure 18. Press System Block Diagram
- Figure 19. Model of the Forge Press
- Figure 20. Three-way Servovalve Block Diagram

- Figure 21. Plots of Experimental and Simulated Ram Velocities
- Figure 22. Plots of Experimental and Simulated Ram Position
- Figure 23. Plots of Experimental and Simulated Ram Load
- Figure 24. Simulation results for small servovalve command and response
- Figure 25. Simulation results for large servovalve command and response
- Figure 26. Forging Design Sequence
- Figure 27. Applied Forging Allowances
- Figure 28. Allowances for Forging Tolerances
- Figure 29. Typical Placement of Length and Width Datum Planes for a Spar Forging
- Figure 30. Typical Placement of Length and Width Datum Planes for a Small Forging
- Figure 31. High Wear Areas for Forging Dies
- Figure 32. Shrinkage and Die Wear Tolerance Application for a Large Forging with Datum Plane Inside Forging
- Figure 33. Shrinkage and Die Wear Tolerance Application for a Small Forging with Datum Plane on Periphery
- Figure 34. Comparison of Geometries to Achieve Mechanical Properties
- Figure 35. Ultrasonic Inspection, near and Far Surface Resolution Problems
- Figure 36. Relationships Between Process Variables and Machine Variables

LIST OF TABLES

- Table I. Examples of Typical Terms for the Optimality Criterion for Microstructure Development During Hot Working
- Table II. Flow Possibilities for a Three-way Servovalve
- Table III. Material Strength as a Function of Cross-sectional Area
- Table IV. Calculated Stress Concentration Factors

FOREWORD

This program is a Phase II SBIR Project to develop simulation-based process design methodologies and tools for intelligently optimizing and controlling metal forming processes. Emphasis is being placed on understanding the evolution of microstructure and the relationships between constitutive relationships (flow stress), the dynamic material model (intrinsic workability) and microstructure development during hot deformation. The research and development approach was based on fundamental concepts that have emerged from control theory and dynamic material modeling. These concepts were used to develop an optimization-based design approach for shape and microstructure optimization.

The work was conducted on-site at the Wright Laboratory /Materials Directorate - Process Design Branch (WL/MLIM) in collaboration with the inhouse research and development team. The technical program was performed under Air Force Phase II SBIR Contract F33615-95-C-5822. Dr. James C. Malas is the Air Force Program Manager. Dr. Harold Gegel is the UES, Inc. Program Manager.

Dr. Dennis Irwin and Mr. Enrique Medina, Austral Engineering & Software, Inc., performed modeling and simulation of metal forming equipment and microstructure development.

Dr. Anil Chaudhary, Applied Optimization (Consultant), developed the concept for a forward-based preform design methodology, and Mrs. Linda Clemens, a Software Consultant, developed the architecture and graphical user interface for dynamic material modeling and data acquisition from remote databases. Mr. Douglas R. Barker, UES, Inc. and his colleagues in the Experimental Processing Laboratory (EMPL) provided assistance during the equipment modeling and

experimental stages of this work. Other WL/MLIM inhouse team members that contributed valuable technical developments and discussions include Dr. W. G. Frazier, Dr. S. Venugopal (NRC Post-Doctoral Fellow), Dr. W. M. Mullins and Mr. Steve Medeiros.

1.0 SUMMARY

The technical objectives of this Phase II SBIR project are as follows:

- To develop robust techniques with feedback for forming process control and optimal process design.
- To develop accurate models and computer simulations of metal forming equipment for the purpose of improving metal forming process design.
- To develop a process design method for controlling microstructure development during hot metal deformation based on modern control theory and state-space models for describing the workpiece behavior and the mechanics of the process.
- To develop a material information acquisition capability from remote databases and standardized materials testing methods that generate information for process simulation and microstructure evolution prediction.

A new process design method for controlling microstructure development during hot metal deformation processes was developed. This approach is based on modern control theory and involves state-space models for describing the material behavior and the mechanics of the process. The challenge of effectively controlling the values and distribution of important microstructural features can now be systematically formulated and solved in terms of an optimal control problem. This method has been applied to the optimization of grain size and certain process parameters

such as die geometry profile and ram velocity during extrusion of plain carbon steel. Various case studies have been investigated, and experimental results show good agreement with those predicted in the design stage. A software product for *Microstructure Trajectory Optimization* was developed, and it is now ready for beta site testing.

Modeling and simulation of metal forming equipment was done to better understand and improve the control of metal forming equipment. Techniques were developed for creating accurate models and computer simulations of metal forming equipment for the purpose of improving metal forming process design. Special emphasis was placed on modeling the dynamic behavior of hydraulic vertical forge presses, although similar principles apply to other types of metal forming equipment.

These principles were applied to modeling and simulation of the 1000 ton forge press in service in the Experimental Material Processing Laboratory (EMPL), Wright-Patterson AFB Ohio.

Experimental verification of the modeling methodology was verified also. These EMPL results indicate that considerable opportunity exists for increasing the life of servohydraulic systems and reducing the cost of maintenance. It was also shown that the press model can be integrated into the finite element method (FEM) for simulating forging processes. This capability allows the process designer to run the forging simulation as a virtual process, making the results very realistic.

A workflow process for precision die design was developed to understand more precisely how optimization-based preform design can be used to improve die design and reduce the cycle time.

The controlling driver in manufacturing is cost reduction for all forged components used to fabricate structures. The focus on forged component manufacturing cost reduction through realistic process design will contribute significantly to the reduction of acquisition costs for new products. This task addressed the aggressive goal for cost reduction and brings focus to the relative processing requirements and cost performance of candidate high strength aerospace and automotive product forms used by OEM's, subcontractors and machining sources in the component manufacturing streams.

A Metallurgists' Notepad software application was developed. This software application allows materials specialists and process engineers to acquire process design data for remote databases using the capabilities offered by the World Wide Web (WWW). The possibility of future implementation of the Metallurgists' Notepad as a fully browser-based intranet application was studied.

Some areas of concern included the following: (a) Computations of Dynamic Material Model Stability Criteria, (b) Database Access, (c) User Training, (d) User Interface, (e) the Development Environment, and (f) Security. Analysis was done to develop a more generalized database structure to support the full range of data retrieval, analysis, export, and reports. A new materials property software application has resulted from this work and will be made available as a commercial product.

2.0 INTRODUCTION

In designing material-working processes for components made of complex structural materials, the most important task is the selection of controlling process parameters, which will ensure the required part quality along with specific mechanical and physical characteristics. The controlling process parameters are the number and sequence of material flow operations, the heat treating conditions, and the associated quality-assurance tests. Special features such as nonlinear, irreversible finite-deformation flow must be considered when designing metal forming operations. Simultaneously, the complex interdependence of the unit process parameters and their effect on finished part quality, reliability, and inspectability must be considered.

An important goal in manufacturing is to determine the optimum means for producing defect-free parts on a repeatable basis. The optimization criteria depend on manufacturing goals and product specifications. The establishment of appropriate criteria requires indepth views — both global and local — of manufacturing processes and material behavior. From an optimization perspective, manufacturing processes require the determination of material flow mechanics to achieve proper process design and to develop a rational strategy for process control. Success in determining this rational strategy depends strongly on understanding the material behavior under processing conditions, and these conditions generally are governed by irreversible thermodynamic processes and inhomogeneous flow behavior.

The modeling of the forging process involves both mechanics and thermodynamics. This process and other metal forming processes, as a rule, are inhomogeneous and transient over a large

volume of the workpiece material, and the material-flow process can be characterized as highly irreversible, dynamic and stochastic in nature. The forging process is dynamical in the sense that it is impossible to precisely define the workpiece material's initial conditions, and it is stochastic in the sense that it is impossible to define when certain metallurgical processes, which provide the necessary degrees of freedom for achieving stable flow, will occur or whether they will occur in series or in parallel. The mechanics of metal forming processes are well established, and numerical methods such as the rigid-thermoviscoplastic and elastic-thermoviscoplastic finite element methods are now being used by industry to analyze two-dimensional and three-dimensional metal forming operations. However, it can be stated that these numerical tools are not being used to their fullest advantage, because most users do not fully understand the interaction of process variables and machine variables in controlling the quality and properties of a finished forging.

The development of an intelligent optimization-based design system is a necessity for minimizing the amount of trial and error design done on the shop floor. The goal is to be able to optimize the metal forming process off-line such that the process design engineer can focus the design effort to finding optimal solutions. The optimization-based design approach will reduce the cycle time for part manufacturing and contribute significantly to the reduction of acquisition costs for new products. It will enable product and process designers to work together in a concurrent engineering mode to make the tradeoffs that may be required between product requirements, die and preform design, process control, quality assurance, heat treatment and machining to achieve an affordable and designer acceptable part.

2.1 PROGRAM OBJECTIVES

The program objectives for this program are directed towards developing an optimization-based design approach for process modeling. These objectives are enumerated as follows:

Develop robust techniques with feedback for forming process control and optimal process design.

Develop accurate models and computer simulations of metal forming equipment for the purpose of improving metal forming process design.

Develop a process design method for controlling microstructure development during hot metal deformation based on modern control theory and state-space models for describing the workpiece behavior and the mechanics of the process.

Develop a material information acquisition capability from remote databases and standardized materials testing methods that generate information for process simulation and microstructure evolution prediction.

2.2 PROGRAM TASKS

Task 1 Develop an Industrial Advisory Committee to direct the flow of the Phase II research from the customer perspective.

Task 2 Standardize Material Testing Procedures to facilitate an accurate calculation of the microstructural evolution models, which are required for coupling with the process model for microstructure control.

Task 3 Development of optimization strategies for equipment control, preform design and microstructure optimization. The driver for these developments will be the requirements posed by the Industrial Advisory Committee.

Task 4 Development of an Interface that will facilitate data and information transfer between the various models such as the equipment model, microstructure model, and control model.

Task 5 Development of an Equipment Servohydraulic System Model. This model will be developed to evaluate the capability of the equipment to deliver the user specified ram velocity, load and energy values.

Task 6 Process Control and Optimal Design Technology Transfer.

2.3 PROGRAM DELIVERABLES

The program deliverables include the following software applications.

- A prototypical Metallurgists' Notepad
- A Microstructure Trajectory Optimization Module
- A Prototype Preform Design Application

3.0 BACKGROUND

One of the most significant barriers for the implementation of simulation-based design technologies in the parts supplier industry has been the requirement of excessive human intervention for process model generation. It is now feasible to draw upon the principles of control and optimization theories and to merge them with computational mechanics to develop a powerful numerical solution strategy for designing a wide range of metal forming processes. The feasibility for accomplishing this overall objective was shown during Phase I of this SBIR project. This work was performed in conjunction with the representatives of aerospace, automotive and hand tool industries. The attention-getting technology needs that the Industrial Advisory Board identified and recommended as high priority research tasks in the Phase II effort are summarized below:

Ram velocity control is needed for controlling microstructure and property evolution, managing the stability of the process, controlling the magnitude of residual stresses. This recommendation came from the aerospace industry.

A methodology should be developed for hammer and screw press energy optimization. Both aerospace and automotive part suppliers and customers made this recommendation.

A methodology for specifying and controlling an optimal ram velocity for simultaneous, multiple station forming. This requirement and recommendation came from the automotive business sector.

A technology need for a process design and manufacturing strategy for controlling the magnitude of residual stresses in precision (netshape) forged parts was recommended. This requirement and recommendation came from the aerospace, automotive, and hand tool companies.

A technology need exists for enhancing die life, including the development of an analysis capability for optimal shrink fit determination. This requirement and recommendation came from the automotive industry.

A capability is needed for achieving press equipment servohydraulic control and optimization. The benefits of this software development application include reducing press maintenance costs, increasing the life of a hydraulic press, and it is the means for implementing optimization-based process design strategies. The automotive industry and primary metal's producers have this requirement and made the recommendation.

The Phase II SBIR project addressed the technology need for ram velocity control, press energy optimization, microstructure optimization, and servohydraulic control of press equipment. The approach used to address these technology needs will be discussed in the report. During the Phase II technical effort, several concepts for preform design were investigated. The approaches taken involved a concept called *idealized material flow*. In this approach, constancy of volume is preserved always. The flow stress of the workpiece material is neglected in the flow analysis, which yields strain-rate trajectories that can be mathematically perturbed to provide a means for satisfying certain desired microstructure evolution criteria and energy minimization requirements. The dynamic material model then introduces real material behavior or workability guidelines selecting

the number of intermediate forging (blocking) stages that are needed for producing the finished forging.

Thus, preform design is a methodology for design is a forging preform that fills the impression zone of the finish die with a minimum amount of energy, while satisfying the temperature and strain-rate criteria for evolving a specified set of microstructures. The process parameters established by this optimization-based design approach also plays an important role in controlling the magnitude of the residual stresses that result. An important aspect of this design approach is that it changes the way a process designer works in designing the tooling and the process. It introduces a direct approach to preform design, which is apposed to a backward approach that is traditionally done. This approach is being pursued as a means for significantly reducing the cycle time for designing and producing netshape forgings.

4.0 SOFTWARE DEVELOPMENT

4.1 METALLURGIST NOTEPAD

The Metallurgist Notepad focuses on Systems Engineering and Thermodynamics for material process design, and features a broad range of usability for both industry and academia. It is a PC-based software tool for accessing and analyzing material data that results from compression testing. Several functions are integrated to produce a complete analysis and design tool. These include:

- Converting raw load-stroke data to flow stress curves
- Adiabatic Temperature Correction
- Viewing microstructure scans
- Dynamic Material Modeling Analysis

Metallurgist Notepad uses an underlying relational database to consolidate test data, graphics files, and analysis results. The database facilitates data access, analysis documentation, and reproducible results. An intuitive user-interface eliminates the need for software-specific training and allows the materials engineer to focus on process design and analysis. Metallurgist Notepad supports the development of database content by providing data import capabilities, and supports other analytical tools by providing data export capabilities. The result is a software application with connectivity to a wide selection of data sources, import/export capability, an extensive selection of analyses and reports, plus an architecture that supports emerging data sources. Metallurgist Notepad has

extensive online help to explain technical concepts, data, and conclusions in easily understood language with ample use of graphics and schematics to illustrate definitions, concepts, and test setups.

4.1.1 Requirements and Design

The requirements and design for Metallurgist Notepad focus on integrating the processes of compression testing, flow stress analysis, adiabatic temperature correction, and creating and analyzing Processing Maps. The need for an intuitive interface, access to material data, and a reproducible analysis process leads to many of requirements identified below.

4.1.2 Usability

Usability for both Industry and Academia is a fundamental requirement with an effect on individual features as well as the fundamental architecture of Metallurgist Notepad. Key usability requirements are listed below:

- Import data from a wide variety of sources, such as text files, spreadsheets, Internet sources, and other databases.
- Export data in formats utilized by other material modeling tools.

- Support browsing, downloading and importing Internet data sources.
- Support dial-up access to non-Internet data sources.
- Employ a flexible architecture to permit incremental software updates when new data sources become available
- Develop an intuitive user interface requiring little or no user training.
- Provide full-service online help functions addressing both software and material process design questions.

4.1.3 Processing Maps

Dynamic Material Modeling is a methodology that produces a “Workability Guide” or Processing Map for materials engineers. Developing this information is a complex process requiring extensive data visibility, user controls, and flexible graphics displays. Interactive tools that related different kinds of material data such as flow curves and microstructure scans are highly desirable. Desired functions for Metallurgist Notepad focus on data verification and validation, flexible display, and reproducibility. Additionally, there is a need to verify and validate the curve fitting algorithms, and identify the sensitivity of results to tolerance factors. Some specific needs include:

- Context sensitive help function focused on technical concepts and definitions for the specific material being analyzed
- Greater control and flexibility of curve fitting routines

- Remove data point outliers interactively while preserving data set reproducibility
- Add capability to view a “banded” range of stability values
- Capability to document the analysis process

4.1.4 Microstructures

Scans of microstructures before and after compression testing reveal actual material behavior.

Interpretation of data analysis is greatly enhanced by viewing microstructure scans that are linked to their respective processing parameters. Metallurgist Notepad will provide for importing microstructure scans into the database, linking them to processing conditions, and viewing the scan independently or “hotkeyed” to Processing Maps.

4.1.5 Data Verification and Validation

The Dynamic Material Modeling methodology is dependent on the quality of data. Data verification will occur during data import and data entry to ensure consistency within the database. Additionally data validation steps are required to evaluate the quality of the flow stress data resulting from compression testing. One important step is to display curves of Log (flow stress) versus $1/\text{Temperature}$ to identify outlying data points and similar curve sets.

4.1.6 Flow Curve Analysis and Adiabatic Temperature Correction

Flow curve data supports Dynamic Material Modeling. The Metallurgist Notepad will provide two important functions here:

- Convert imported load-stroke data to flow stress curves and stores those curves in the database
- Perform Adiabatic Temperature Correction on flow stress curves and store the resulting curves

4.1.7 Data Import and Export

The Metallurgist Notepad will access a wide variety of data sources in order to build its database. The database may be built using data from a variety of sources, such as HOTCOMP, text files, MME files, NCEMT files. This capability is essential for providing support to a wide range of users. These databases may be located on a local network, on the Internet, or on a dialup computer source. Metallurgist will also provide the capability to export data to other software programs utilizing flow stress or DMM data, such as the Microstructure Optimization software.

4.1.8 Material Processing Database

The Metallurgist Notepad features an Open Database Connectivity (ODBC) standard relational database. Microsoft Access is the current database engine. The ODBC standard ensures compatibility with other ODBC databases and related software. The relational aspect of the database ensures flexible growth and features. The database effectively becomes a repository of data with the potential for both wide access and security management.

4.1.9 Software Architecture

The Metallurgist Notepad is being developed in Microsoft's Windows 95 platform and should perform well with Windows NT 4.0 or later versions. Microsoft's Visual Basic was selected as the development language in order to facilitate:

- Rapid development,
- Object oriented design,
- Database connectivity,
- Multi-language development compatibility, and
- Internet compatibility.

Microsoft Access is the current database management tool. MS-Access is ODBC compliant, and compatible with many Internet tools. The Metallurgist Notepad uses Olectra Chart by KL Group for graphics application support. Olectra is compatible with multiple languages in the Windows 95/NT environment and has parallel products in the Unix environment. It also features WWW capability, and supports a wide variety of native graph types, plus thorough programmatic control over graph properties and actions.

4.1.10 Current Status

Much of the work to date has focused on developing the requirements and design of Metallurgist Notepad, building a prototype to demonstrate basic ideas, then proceeding to an initial software product and corresponding database. Metallurgist Notepad has developed a user interface for supporting the requirements and design discussed above. Additionally, Metallurgist Notepad has developed several capabilities:

- Views flow stress curves in tabular and graphic format from data stored in a relational materials database.
- Views microstructure scans stored in a relational database.
- Imports MME files and stores them in the database.
- View MME Data, and control the display of maps. (See Figure 1)
- Produce Stability Maps using the ANTARES algorithms. (See Figure 2)

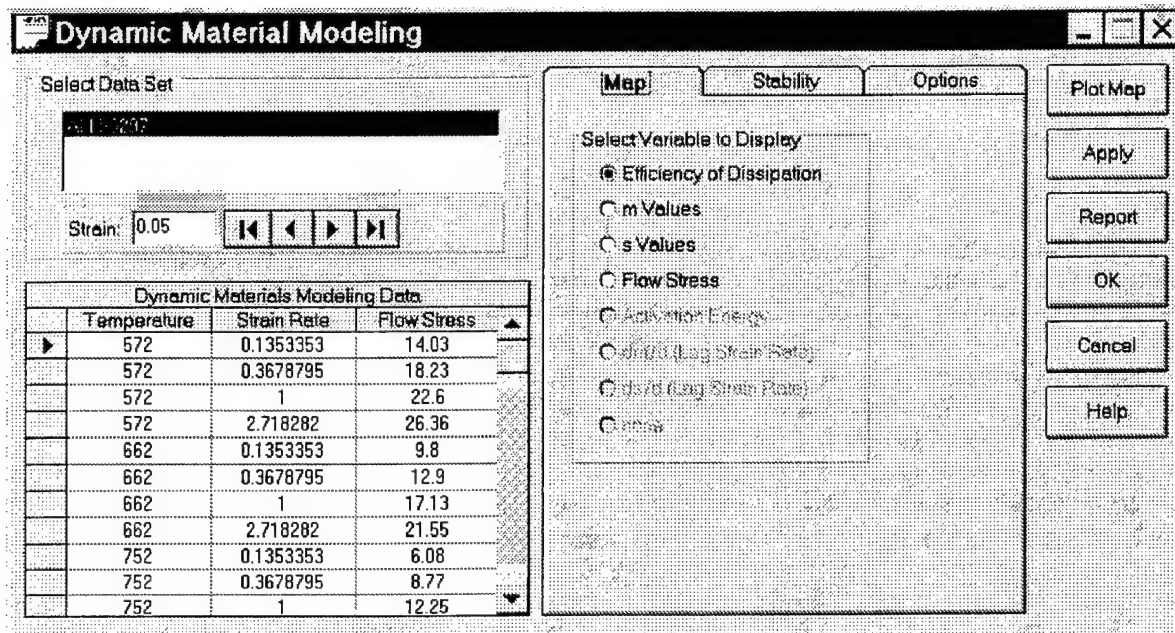


Figure 1. View of MME Data, and Control of Data for Maps

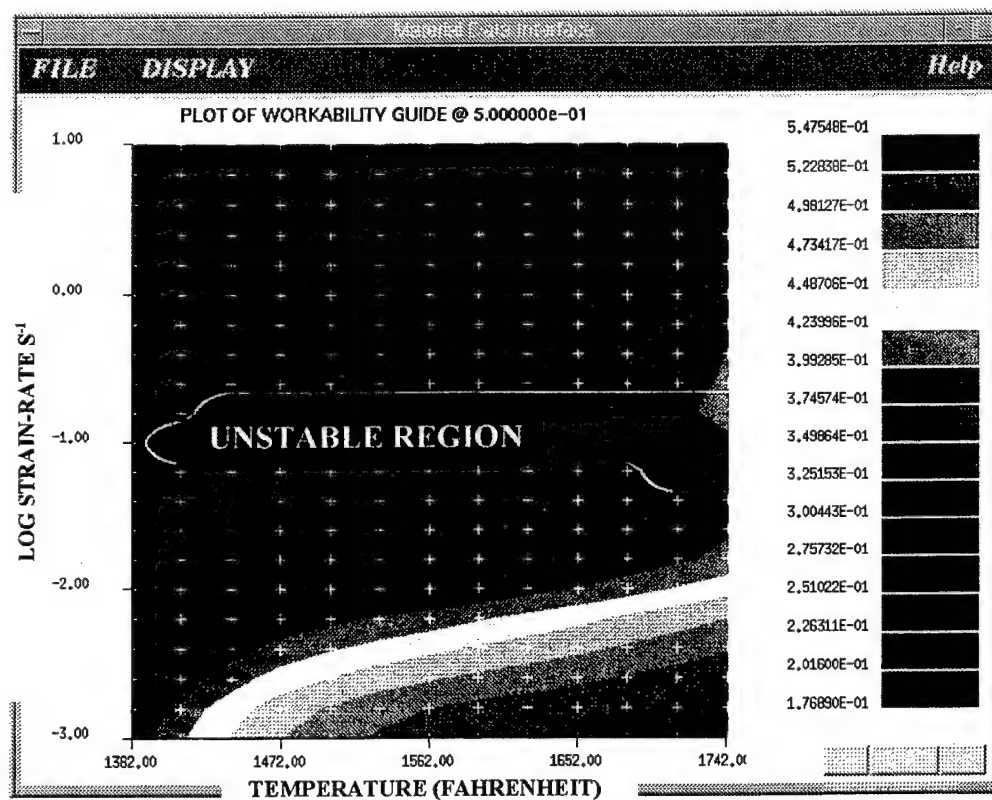


Figure 2. Dynamic Material Ti-6Al-4V Structurally Porous Material (SPM)

4.1.11 Future Development

The next step for Metallurgist Notepad is to move from the demonstration program to a fully capable software program which implements the full range requirements and design described above. The development scope is outlined below:

- I. Database Development
 - A. Identify all required database elements (partially accomplished) and relationships
 - B. Complete the design of a database structure
- II. Flow Stress analysis (implement HOTCOMP algorithms)
- III. Adiabatic Temperature Correction (implement HOTCOMP algorithms)
- IV. Dynamic Material Modeling
 - A. Complete implementation of algorithms
 - B. Extensive verification and validation

- C. Documentation of algorithms
- D. Hotkey interface for labeling, and data display
- E. Data verification functions (log flow stress v. Temperature, etc.)
- F. Evaluate a possible experimental design wizard and data clustering issues

V. User Interface

- A. Develop all dialog boxes and enhance hotkey functions
- B. Tie-in to Internet

VI. Data Import/Export

- A. Implement wide range of data import source, local and remote
- B. Ensure data verification during import
- C. Support identified software with file export

VII. User Assistance

- A. Online help for software issues

- B. Online help for engineering/materials issues
- C. Develop material specific online help

VIII. Internet

- A. Analyze a possible future implementation of Metallurgist Notepad as a fully browser-based Intranet application – incorporating Java, C, ActiveX, Internet Relay Chat (IRC), ODBC database, and multi-media elements.
- B. Areas of concern include: computational efficiency, Access database, user Training, user interface, development environment, and security.

4.2 MICROSTRUCTURE OPTIMIZATION

4.2.1 Introduction

The development of optimal design and control methods for manufacturing processes is needed for effectively reducing part cost, improving part delivery schedules and producing specified part quality on a repeatable basis. Existing design methods are generally *ad hoc* and lack adequate capabilities for evaluation of the effects of primary process parameters such as deformation rates,

die and workpiece temperatures, and tooling system configuration on the manufacturing process and on the final product. This situation presents major challenges to process engineers who are faced with ever increasing constraints on cost, quality and growing production requirements for near net-shape components with controlled microstructures and properties. It is important to develop new systematic methodologies for process design and control based upon scientific principles which sufficiently consider the behavior of the workpiece material and the mechanics of the manufacturing process.

A new strategy for systematically calculating near optimal control parameters for hot metal deformation processes is presented. This approach is based on modern control theory [1] and involves developing state-space models for material behavior and hot deformation processes. In this strategy, control system design is carried out in two basic stages. Analysis and optimization are performed in both stages. In the first stage, the kinetics of certain dynamic microstructural phenomena and the intrinsic hot workability of the metal alloy system are used, along with an appropriately chosen optimality criterion, to calculate nominal strain, strain-rate, and temperature trajectories (histories) that will cause the microstructure at a given location in a workpiece to evolve from its initial state, through an acceptable path, to the desired final state. These nominal trajectories are valid for different hot deformation processes (forging, rolling, extrusion, etc.) and are thus independent of die geometry and flow pattern. A suitable process simulation model is then used in the second stage to calculate process control parameters, such as ram velocity profiles and billet temperature, which best achieve, in selected areas of the workpiece, the nominal strain, strain-rate, and temperature trajectories calculated in the first stage.

An application of the new process design approach to a round-to-round hot metal extrusion process is looked into in this paper. An extrusion process was selected for study in this work due to the following reasons: (1) extrusion typically involves large deformation with large variations in strain-rate; (2) relatively simple analytical models are available for describing the process; and (3) strain and strain-rate trajectories can be effectively controlled via optimized design of die geometry. In the following sections, the development of the two-stage optimal design approach, along with its application to the design of an extrusion process is presented. Case studies, as well as an experimental validation of the procedure, are also presented.

4.2.2 Description of Direct Extrusion

Extrusion is a process by which the cross section of a billet is reduced by forcing it to flow through a die. In a typical direct extrusion process, shown in Figure 3., a billet is placed in a chamber and the force exerted by the ram makes the metal flow through the die. The process is used to manufacture both finished and semi-finished products. As a

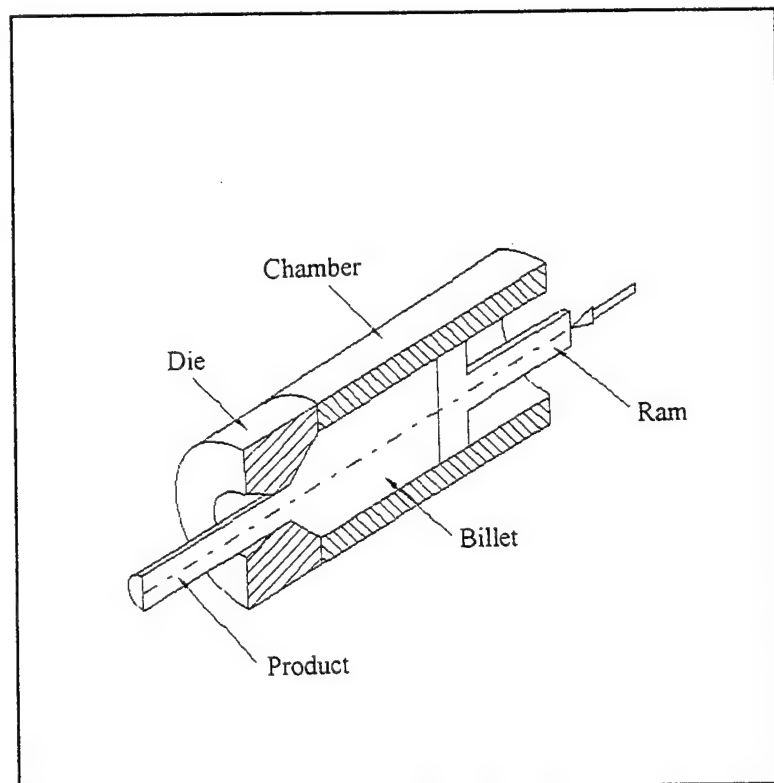


Figure 3. Extrusion Process

primary processing operation, extrusion is used to refine the large grain cast structure. The extruded product is then in a condition more amenable to final shape making by other metal forming operations. The refinement of grains during extrusion is influenced by several factors including the initial temperature of the billet, the reduction in area, and the strain-rate variation that the material experiences during deformation.

Hot extrusion is usually carried out using converging dies, in which the cross section of the die orifice changes gradually from the initial billet shape to the final product shape over the length of the die. The strain and strain-rate variation that the material experiences as it flows through the die depends on the die profile. Conical die, constant strain-rate die and cubic streamline die are examples of die configurations commonly used in industry.

4.2.3 Microstructural Evolution During Hot Deformation

Microstructural changes which occur during hot deformation are consequences of complex metallurgical phenomena such as recovery, recrystallization, grain growth, phase transformations, and precipitation and dissolution reactions. These phenomena may occur dynamically during hot deformation processing or statically during post-deformation cooling or heat treatment. The mechanisms and kinetics of these phenomena, as well as, the associated changes in size, morphology, distribution, volume fraction, and composition of the constituent phases are strongly dictated by the macroscopic heat-flow and material-flow processes. While the temperature distribution in the workpiece is controlled primarily by the interface heat transfer between the

workpiece and the dies, frictional-heating and deformation-heating effects also contribute significantly. At the same time, the distributions of strain, strain-rate, effective stress, and hydrostatic stress within the deforming body are influenced by the material-flow behavior as well as the thermal history.

Dynamic recrystallization is commonly observed in hot extrusion processes which involve very large strains (typically true plastic strain $\epsilon > 0.5$). Metals and alloys characterized by relatively low-stacking-fault energy (e.g., copper, nickel, austenitic steels) have a high propensity for undergoing restoration via dynamic recrystallization. Under hot-working conditions, these materials exhibit flow curves containing single maxima. A schematic representation of a typical microstructure evolution during dynamic recrystallization is shown in Figure 4. When the plastic strain exceeds a

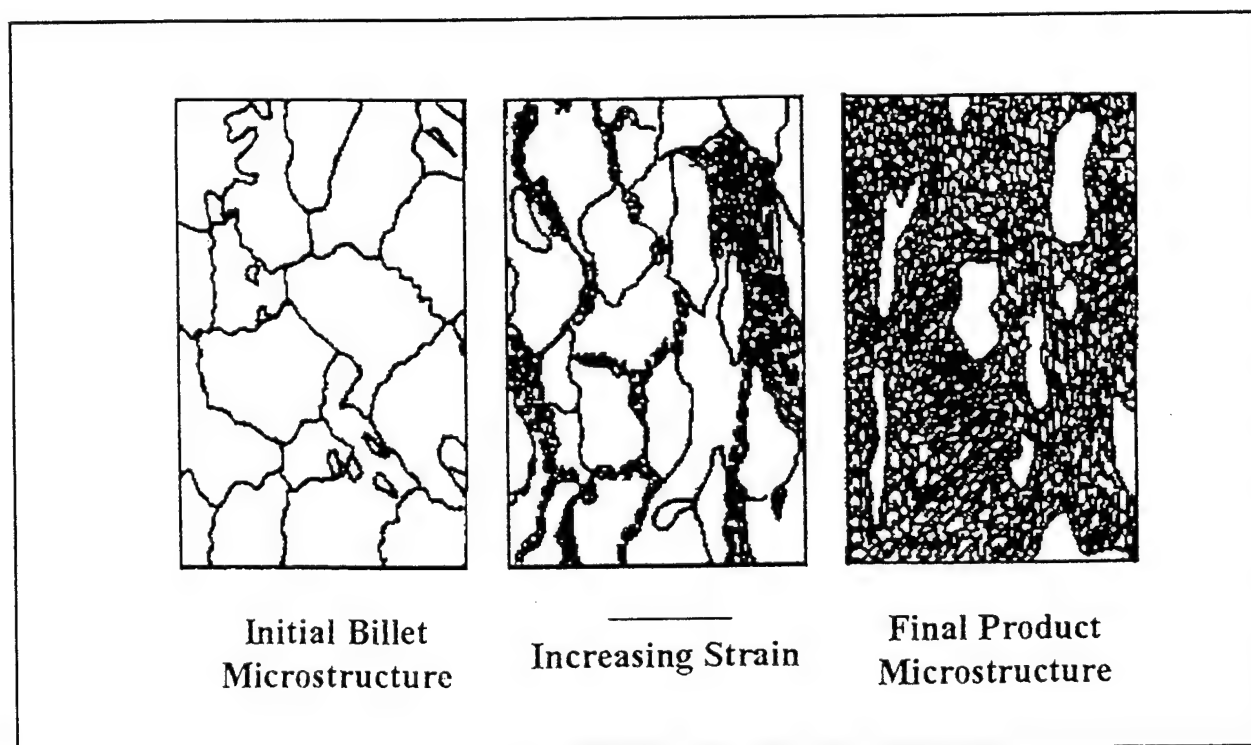


Figure 4. Schematic Representation of Dynamic Recrystallization

critical value, ε_c , dynamically recrystallized grains nucleate. Additional deformation results in a replacement of the unrecrystallized structure by a completely recrystallized structure. This transition from unrecrystallized to recrystallized microstructure is strongly dependent on processing conditions and may occur over a relatively small increment in deformation.

4.2.4 The Two-Stage Approach to Optimal Control of Deformation Processes

The process design and control strategy presented in this paper requires three basic components for defining and setting up the optimization problem: (1) a dynamical system model, (2) physical constraints, and (3) an optimality criterion. In metal forming, the system models of interest are material behavior and deformation process models; constraints include the hot workability of the workpiece and the limitations of the forming equipment. Optimality criteria could be related to achieving a particular final microstructure, regulating temperature, and/or maximizing deformation speeds.

The present two-stage approach decomposes the analysis and optimization into a workpiece material behavior control problem and a process mechanics control problem. Since optimization methods are used in both design stages, the two stages are also called *microstructure development*

optimization and process optimization in the block diagram of Figure 5.

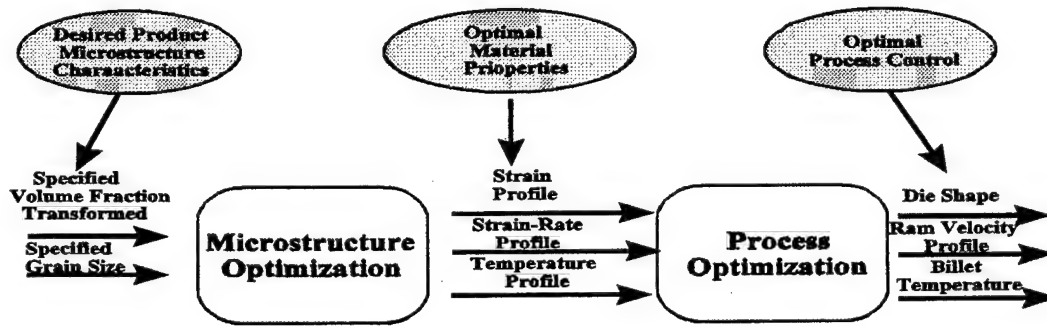


Figure 5. Block Diagram of the Two-Stage Approach

The microstructure development optimization determines optimal trajectories of strain, strain-rate, and temperature $T(t)$. From these optimal material trajectories, the process optimization stage determines optimal process control parameters, namely the die shape, the ram velocity profile $V_{ram}(t)$, and the billet temperature $T_{billet}(t)$. The goals of the first stage are to achieve enhanced workability and to obtain prescribed microstructural features in the deformed workpiece. In the second stage, a primary goal is to achieve the thermomechanical conditions obtained from stage one for predetermined regions of the deforming workpiece. It is recognized that this two-stage

approach yields idealized process control solutions that could be further improved with advanced feedback methods.

4.2.5 Material Behavior and Process Modeling Issues

The effectiveness of the two-stage approach presented in this paper is largely dependent on the availability and reliability of models for the behavior of the material and for the metal forming process. In the first stage, material behavior models that describe the kinetics of primary metallurgical mechanisms such as dynamic recovery, dynamic recrystallization, and grain growth during hot working are required for analysis and optimization of material system dynamics. These mechanisms have been studied extensively for a wide range of metals and alloys [2-5]. The relationships for describing particular microstructural processes have been developed and reported for conventional materials such as aluminum, copper, iron, nickel, and their dilute alloys, with steel receiving the most study. It has also been suggested that, for certain ranges of temperature and strain-rate, the deformation mechanisms of specialty alloys such as superalloys, intermetallics, ordered alloys, and metal matrix composites become well defined and are amenable for modeling [6,7].

As an illustration of a material behavior model, consider the case of a material that undergoes

dynamic recrystallization during hot deformation. A possible state-space model is given by

$$\begin{bmatrix} \dot{d} \\ \dot{\chi} \\ \dot{\epsilon} \\ \dot{T} \end{bmatrix} = \begin{bmatrix} f_1(T, \dot{\epsilon}, d) \\ f_2(T, \dot{\epsilon}, d, \chi) \\ \mu \\ \frac{\eta \sigma \dot{\epsilon}}{\rho C_p} \end{bmatrix} \quad (1)$$

where d is grain size, T is temperature, ϵ is strain, μ is strain-rate, χ is percent recrystallized, f_1 and f_2 are pre-specified functions, η is a coefficient that determines how much work is converted into heat σ , is flow stress, and the product ρC_p is the heat capacity of the material. Note that the system input μ is the strain-rate for this model. The trajectories followed by the state variables d , χ , ϵ , and T , which are dictated by their initial conditions and by the trajectory followed by the system input—in this case the strain-rate — determine the evolution of the material microstructure during deformation.

In several industries, process modeling has reached a high level of sophistication and acceptance as a process analysis tool. Current process models are capable of analyzing fairly complex material flow operations such as three-dimensional, nonisothermal deformation processes with a sufficiently high degree of accuracy. For example, in the forging industry, detailed numerical analyses of the phenomenon of the workpiece filling the forging die, the resulting die stresses, and the post-deformation heat treatment of the workpiece are applied for verification of forging and heat treatment process designs [8,9].

4.2.6 Material Behavior Constraints and Optimality Criteria

In addition to dynamic system models, the formulation of an optimal control problem requires a statement of physical constraints and specification of an optimality criterion. The limiting process conditions for acceptable hot workability are important material behavior constraints in the first stage of the control strategy. Several methods for identifying acceptable strain-rate and temperature ranges for hot working metal alloys have been presented in scientific literature. These include material flow stability analysis [6,7], deformation maps [8], and damage nucleation maps [9]. Within the acceptable processing regime of temperature and strain-rate variations, a particular thermomechanical trajectory is determined using the prescribed optimality criterion such as producing specified hot worked microstructural characteristics.

4.2.7 General Formulation of the Optimal Control Problem

Following the description above, the design problem is formulated here into an open-loop optimal control problem that can be stated as follows: Find u to minimize the optimality criterion

$$J = h(\chi(t_f)) + \int_0^{t_f} g(\chi(t), u(t)) dt \quad (2)$$

while satisfying the system state equation

$$\dot{\chi}(t) = f(\chi(t), u(t), \chi(0) = \chi_0 \quad (3)$$

In the equations above, t is time, $x(t)$ is a vector of state variables, u is the system input, t_f is the duration of the deformation process, h is a penalty function associated with violating the desired final state, g is the integrand of the penalty associated with the trajectories followed by the state variables and the input, f is a vector function that describes the process dynamics, and x_0 is the initial state vector. In this context, the term *final state* or *final value* refers to the value of the state vector or the variable of interest at the end of processing, while the term *trajectory* refers to a history of the values attained by the variable under consideration during processing.

4.2.8 Optimality Criteria for Microstructure Development

Careful selection of optimization criteria is a crucial task for finding the most appropriate design solutions. In the control of microstructure development during hot metal deformation, design criteria include the requirement of producing specified microstructural features and/or gradient of microstructure within a given variance on a repeatable basis. These objectives and others can usually be formulated as functions to be minimized, and are often lumped together into a single scalar optimality criterion J in the form

$$J = J_1^F + J_2^F + \dots + J_{n_f}^F + J_1^T + J_2^T \dots J_{n_t}^T \quad (4)$$

where the superscripts F and T refer to requirements on desired final states and trajectories, respectively, and n_F and n_T refer to the total numbers of such specifications. In the case where it is desired that microstructure feature x achieve a value x_d at the termination of the deformation process, the corresponding term in J often has the form

$$J_i^F = \beta_i (\chi(t_f) - \chi_d)^2 \quad (5)$$

where β_i is a weighting factor. This type of function can also be used to include certain fixed process parameters and other values for non-microstructural quantities, such as strain and temperature, in the optimization calculations. The terms in the optimality criterion define requirements on the trajectories followed by the state variables and control inputs during the forming process, and have integral forms.

Table I shows some examples of typical optimality criteria for microstructure development during hot deformation. Both final value and trajectory specifications have been included. The general formulation of this approach allows new terms to be defined according to the specific needs of each design problem. The quantities $f(x;a)$ and $f(x,a,b)$ in Table I are penalty functions that can be used to constrain optimized design solutions to stay within acceptable process parameter ranges for satisfactory material workability or to stay within the capabilities of the forming equipment. These functions evaluate to virtually zero for values of x in the acceptable range and attain very high values when x is outside that range. Scalars a and b define the acceptable ranges for process

parameters such as temperature or strain-rate. An example of a penalty function is shown in Figure 6.

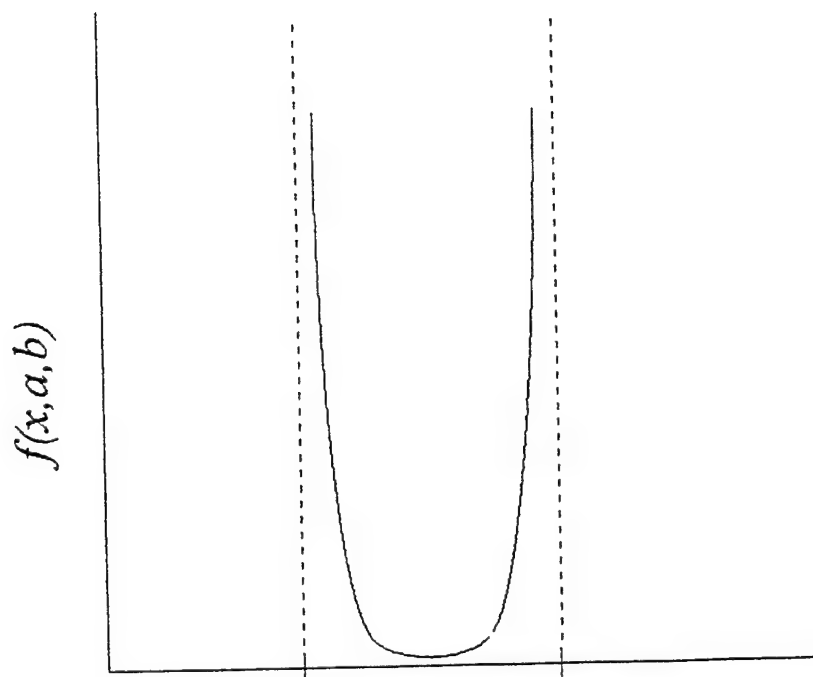


Figure 6. Penalty Function ($f(x, a, b)$) for Constraining Process Parameters between a and b

The weight factors serve three purposes. First, weight factors are used to scale various J -terms so that they have comparable influence in the overall optimality criterion. Second, weight factors are increased for certain J -terms according to their relative importance to achieving overall design requirements. Third, weight factors may be adjusted in order to avoid possible conflicts in design requirements and obtain a satisfactory compromise solution.

4.2.9 Solution of the Microstructure Development Trajectory Optimization Problem

The approach used in obtaining a solution to the optimization problem described above depends on two developments. First, a set of necessary conditions for optimality is obtained by applying variational calculus principles [1]; this formulation transforms the optimization problem to a problem of solving a set of constraint equations. Next, a search-based numerical algorithm is developed for the solution of these equations. Details of the algorithm formulation are given by Frazier [10].

4.2.10 Application Of The Two-Stage Optimization To Steel Extrusion

Results of the application of the two-stage approach to the optimization of a steel extrusion process are presented in this section. A state space model for microstructural response was formulated from available β_1 microstructural models. The optimization algorithm was then applied to obtain controlled grain sizes through hot extrusion of plain carbon steel.

4.2.10.1 Models for Dynamic Recrystallization of Steel

The application of the proposed microstructure development optimization approach depends on the existence of a state-space model that describes how the microstructure changes in time as a function of various process parameters. Microstructural evolution during hot deformation of steel can be described in terms of changes in quantities such as grain size and volume fraction transformed as

functions of process parameters such as strain, strain-rate, and temperature. Many such descriptions for hot deformation of steel have been developed, and have been summarized by Kumar et al. [11]. For this study, a model developed by Yada et al. [12, 13, 14] to describe the effects of strain, strain-rate, and temperature on the microstructural changes during hot rolling of steel was used. According to this model, the volume fraction recrystallized χ evolves according to the expression

$$\chi = 1 - \exp \left[\ln(2) \frac{(\varepsilon - \varepsilon_c)^2}{\varepsilon_{0.5}} \right], \quad (6)$$

where

$$\begin{aligned} \varepsilon_c &= 4.76 \times 10^{-4} \exp \left(\frac{8000}{T} \right) \\ \varepsilon_{0.5} &= 1.144 \times 10^{-5} d_0^{0.28} (\dot{\varepsilon}^{0.05}) \exp \left(\frac{6240}{T} \right) \end{aligned} \quad (7)$$

Note that χ is primarily dependent on the imposed strain, ε . The volume fraction recrystallized is essentially zero until a critical value of strain, ε_c . Beyond this strain, recrystallization proceeds rapidly along an "S" type curve; complete recrystallization occurs with very little additional deformation. The kinetics of the recrystallization are described by the amount of additional strain required to cause 50% recrystallization ($\varepsilon_{0.5}$). In Equation 7, $\varepsilon_{0.5}$ is very small and complete recrystallization occurs almost instantaneously after the critical strain. The volume fraction recrystallized also depends upon strain-rate $\dot{\varepsilon}$, temperature T , and initial grain size d_0 , through their

influence on ε_c and $\varepsilon_{0.5}$. However, this dependence is negligible. The average grain size d obtained after recrystallization is given, as a function of only strain-rate and temperature, by

$$d = 22,000 (\dot{\varepsilon})^{-0.27} \exp\left(-0.27 \frac{Q}{RT}\right) \quad (8)$$

where $Q = 267$ kJ/mol is the activation energy and R is the universal gas constant. Equations 6 and 8 were developed for deformation at constant strain-rate and temperature.

These equations imply complete recrystallization occurs instantaneously. Therefore, during large deformations, it is reasonable to assume that beyond the critical strain successive recrystallizations occurs for strain increments equal to the critical strain. Furthermore, since grain size depends upon strain-rate and temperature, each recrystallization step will result in changes in average recrystallized grain size which will depend upon the current deformation conditions.

In order to transform Equation 6 into a form that can be used in the state equation framework, it is assumed that the volume percent recrystallized is not sensitive to the rate of change of strain-rate nor the rate of change of temperature. The chain rule of differentiation can then be applied to Equation 6 to obtain which is a dynamic equation for the time derivative of the volume fraction

recrystallized. This equation is correct to first order.

$$\dot{\chi} = \frac{\partial \chi}{\partial \varepsilon} \frac{\partial \varepsilon}{\partial t} = \frac{2 \ln 2}{\varepsilon_{0.5}^2} (\varepsilon - \varepsilon_c) (1 - \chi) \dot{\varepsilon} \quad (9)$$

During deformation, most of the mechanical work exerted on the workpiece transforms into heat, and this results in an increase in temperature. The equation for the rate of change of temperature due to deformation can be easily shown to be

$$\dot{T} = \frac{\eta \sigma \dot{\varepsilon}}{\rho C_p} J^T, \quad (10)$$

where the flow stress σ is a function of strain, strain-rate and temperature given by [13]

$$\begin{aligned} \sigma &= \sinh^{-1} \left(\frac{\dot{\varepsilon}}{A} \right)^{\frac{1}{n}} \exp \left(\frac{Q}{RT} \right) / 1.15 \times 10^{-5} \text{ kPa} \\ \ln A &= \frac{13.92 + 9.023}{\varepsilon^{0.502}} \\ n &= \frac{-0.97 + 3.787}{\varepsilon^{0.368}} \\ Q &= \frac{125 + 133.3}{\varepsilon^{0.393}} \text{ kJ/mol} \end{aligned} \quad (11)$$

In Equation 10, η is the fraction of mechanical work converted to heat, and is generally about 0.95.

The state space model for the chosen steel, which gives the evolution in time of volume fraction recrystallized, strain and temperature can be summarized as follows:

$$\begin{bmatrix} \dot{\chi} \\ \dot{\varepsilon} \\ \dot{T} \end{bmatrix} = \begin{bmatrix} \frac{2 \ln 2}{\varepsilon_0^{0.5}} (\varepsilon - \varepsilon_c)(1 - \chi) \dot{\varepsilon} \\ u \\ \frac{\eta \sigma \mu}{\rho C_p} \end{bmatrix} \quad (12)$$

$$d = 22,600 \mu^{-0.27} e^{\frac{-0.27Q}{RT}} \quad (13)$$

As previously mentioned, the evolution of strain is completely determined by the strain-rate, which is the system input, i.e., $\mu = \dot{\varepsilon}$. The average grain size after recrystallization given in Equation 13, which is the same as Equation 8, is treated as an output of the dynamical system in the sense that it does not influence the evolution of strain, temperature or the volume fraction, which has recrystallized. Therefore, it does not need to be included as one of the state variables.

4.2.10.2 First Stage: Formulation of a Cost Functional and Trajectory Optimization

Since the microstructure of a material directly influences its mechanical properties, control of microstructural features is of primary concern in the design of deformation processes. Therefore, the cost functional should place a significant emphasis upon the final microstructural state of the

material. In addition, it is also important that the path followed by the material during the deformation process remain within certain bounds to avoid undesirable events from occurring. Unacceptable designs may be due to failure of the material; for example, cracking can occur if the process is not designed to stay within ranges of acceptable material workability. It would also be unacceptable to calculate material trajectories that cannot be obtained in practice because of limitations in the capacity of the equipment. By including material and equipment limitations into the optimality criterion, these difficulties can be prevented. Table I lists several types of terms that can be included in the optimality criterion to account for design constraints.

Table I. Examples of Typical Terms for the Optimality Criterion for Microstructure Development During Hot Working

Design Objective	Term in the Optimization Criterion
Achieve final average grain size χ_d	$J_i^F = \beta_i (\chi(t_f) - \chi_d)^2$
Achieve final strain of ε_1	$J_i^F = \beta_i (\chi(t_f) - \chi_d)^2$
Maintain Strain-Rate between u_1 and u_2	$J_j^T = \int_0^{t_f} \beta_j(t) f(u, u_1, u_2) dt$
Limit deformation heating; initial temperature is T_0	$J_j^T = \int_0^{t_f} \beta_j(t) (T - T_0)^2 dt$
Keep strain rate under u_1 because of equipment limitations	$J_j^T = \int_0^{t_f} \beta_j(t) f(u, u_1) dt$
Maintain temperature between T_1 and T_2 because of workability considerations	$J_j^T = \int_0^{t_f} \beta_j(t) f(T, T_1, T_2) dt$
Limit energy consumption; $u^2(t)$ is a measure of power	$J_j^T = \int_0^{t_f} \beta_j(t) u^2(t) dt$

For the extrusion case studied in this effort, the optimality criterion was formulated so as to attain a final strain of 2.0, while maintaining the average recrystallized grain size at a desired value of 26 μ m throughout the process. With these requirements, the optimality criterion is given by

$$J = 10(\varepsilon(t_f) - 2.0)^2 + \int_0^{t_f} (d(t) - 26)^2 dt. \quad (14)$$

The weighting factor of 10 for the term that penalizes deviations from the desired final strain was selected by comparing the results of several trials in which different weights were used.

The trajectory optimization algorithm was successfully applied to this problem, and the results are presented in the solid lines marked as *CASE 1* in Figures 7, 8 and 9. These figures show the optimal strain-rate, temperature and strain trajectories. Figure 10 shows the corresponding change in recrystallized grain size, as predicted by the model. The initial grain size for the material was approximately 180 μ m. The solid vertical line at the beginning of the average grain size trajectory corresponds to the change in grain size which occurs when the first recrystallization takes place at a strain of approximately 0.25. Figures 7 - 10 also show additional optimal design cases for desired final grain sizes of 30 μ m (*CASE 2*) and 15 μ m (*CASE 3*). The initial temperature for *CASE 1* and *CASE 2* was 1273K; for *CASE 3* it was 1223K. It is worth noting that Figures 9 and 10 show that the desired recrystallized grain size trajectory and final strain are obtained in all three cases.

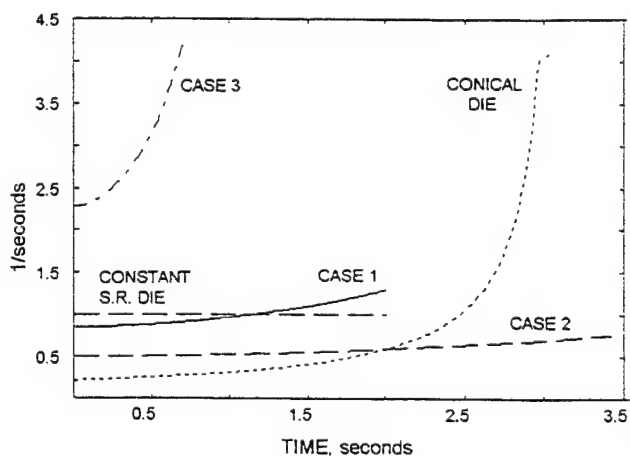


Figure 7. Strain-Rate Trajectories

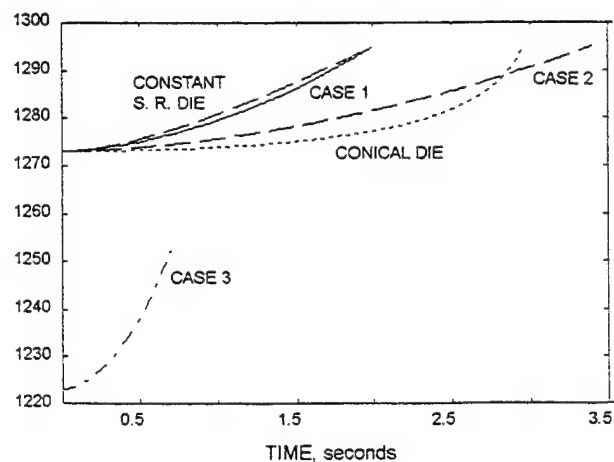


Figure 8. Temperature Trajectories

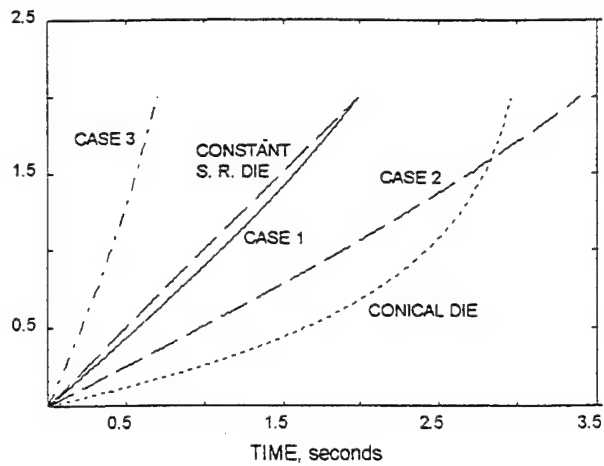


Figure 9. Strain Trajectories

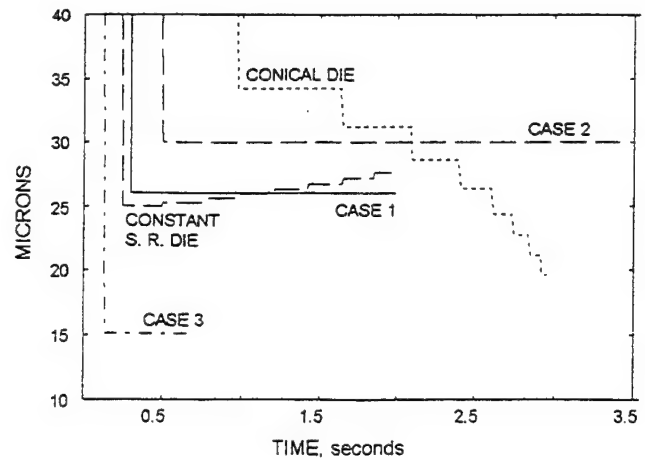


Figure 10. Recrystallization Grain Size Trajectories

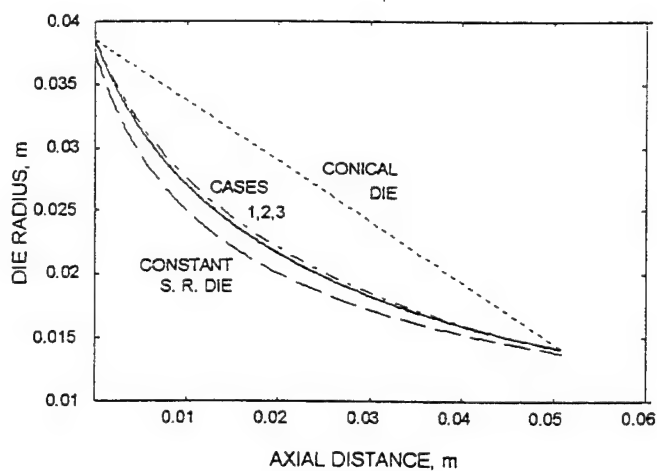


Figure 11. Die Profiles

4.2.10.3 Stage Two: Process Mechanics Control and Optimal Die Design

In a metal forming operation, the trajectories of the various parameters (i.e., strain, strain-rate, temperature, etc.) that influence microstructure are the result of the combined effects of all

deformation process parameters, such as the die and workpiece geometry, die and workpiece temperatures, and ram velocity. The second stage of the optimal design problem involves identifying the process parameters that can deliver the desired trajectories identified in the first stage. Generally, all points in the deforming piece will not follow the same strain, strain-rate, and temperature trajectories. Therefore, the deformation process parameters may have to be designed in order to ensure that selected critical areas of the workpiece experience the designed trajectories. In principle, a second optimization problem can be formulated that determines values for process parameters to achieve the desired trajectories at pre-determined points in the workpiece. Such an approach would require a simulation of the deformation process, by slab-analysis, FEM etc., for each evaluation of the objective function.

In this example, extrusion has been chosen as the deformation process. For a round-to-round extrusion, it is possible to analytically calculate the die shape and ram velocity necessary for achieving the desired strain and strain-rate profiles at the center line of the workpiece, using slab analysis. If r_0 is the initial radius of a cylindrical billet, L is the die length, and t_f is the time required by a slab of material to traverse the length of the die, the ram velocity can be computed from the strain trajectory $\varepsilon(t)$ as follows:

$$V_{ram} = \frac{L}{\int_0^{t_f} (\exp \varepsilon(t) dt)} \quad (15)$$

The shape of the die, expressed as radius r and axial position y , for different locations along the strain trajectory can be calculated as follows:

$$r(t) = r_0 \exp\left(\frac{-\varepsilon(t)}{2}\right) \text{ and } y(t) = V_{ram} \int_0^t \exp \varepsilon(t) dt . \quad (16)$$

The optimal die profiles shown in Figure 11 were obtained by using this approach. The corresponding ram velocities are 8.43 mm/s for *CASE 1*, 5.0 mm/s for *CASE 2*, and 25.1 mm/s for *CASE 3*. The die shapes for the three cases discussed are almost coincident. Since the die shape is almost the same for the three optimization cases considered, one can achieve different recrystallized grain sizes simply by changing the velocity of the extrusion ram and the initial billet temperature. Also worth noting is that the three optimal die shapes are almost identical to that of the constant strain-rate die.

4.2.10.4 Comparison with Standard Die Designs

In addition to the three optimal design cases discussed above, Figures 7 - 10 also show the trajectories of the strain, strain-rate, temperature and recrystallized grain size for two standard converging dies: the conical die and the constant strain-rate die. The profiles of these standard dies are included in Figure 11. Both these dies result in the same final strain of 2.0, but the trajectories are quite different. The constant strain-rate die, as the name suggests, maintains a constant strain-rate (CSR) throughout the length of the die, while the strain-rate experienced by the workpiece during extrusion through a conical die starts at a very low value at the beginning of extrusion and

increases by almost one order of magnitude at the end Figure 7. The plots assume a ram velocity of 8.43 and 8.0 mm/sec for the CSR and conical dies, respectively. In Figure 10, the recrystallized grain size trajectories for these two die shapes show step changes. These correspond to successive dynamic recrystallizations.

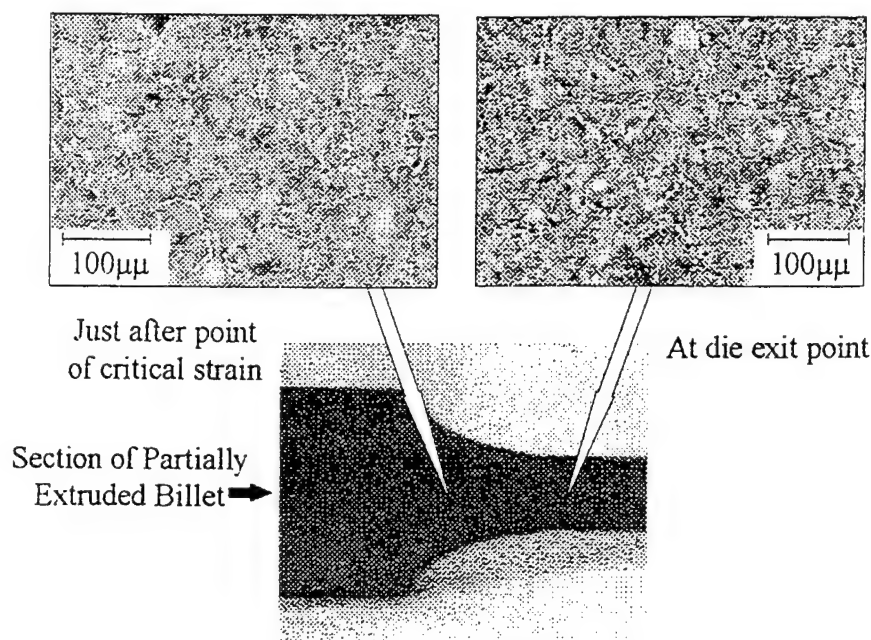


Figure 12. Microstructures at Location of (first) Critical Strain and Die Exit

The strain-rate using the die in *CASE 1* begins slightly below that for the CSR die, but increases to a value slightly higher than that for the CSR die by the end of extrusion. Figure 8 shows that the temperature rise for the CSR die is equal to that for *CASE 1*, while Figure 10 shows that the final recrystallized grain size for the CSR die is slightly larger than that for *CASE 1*. These observations can be rationalized as follows. According to Equation 8, the final recrystallized grain size is influenced by two factors: the temperature and the strain-rate. Under isothermal conditions, at a constant strain-rate, the recrystallized grain size will be constant once the critical strain is exceeded.

However, during any deformation process, some increase in temperature occurs due to the conversion of mechanical work into heat. At a constant strain-rate, this results in a gradual increase in recrystallized grain size with each successive recrystallization. This increase in recrystallized grain size is seen as steps in the grain size trajectory for the CSR die in Figure 10. The die designed in *CASE 1* compensates for this increase in recrystallized grain size by gradually increasing the strain-rate as seen in Figure 7. The result is the constant recrystallized grain size of 26 μ m seen in Figure 10. In the case of the conical die also there is an increase in temperature due to deformation heating, but the simultaneous increase in strain-rate is substantially greater. As a result of this, the recrystallized grain size decreases with each successive recrystallization.

An extrusion die of with the shape obtained from *CASE 1* of the trajectory optimization algorithm was fabricated from H-13 tool steel. A billet of AISI 1030 steel was extruded with a 6000 kN Lombard horizontal extrusion press located at Wright-Patterson Air Force Base, Ohio. The initial temperature of the billet was 1273K and that of the extrusion chamber, die and follower block was 533 K. A ram velocity of 8.43 mm/sec was used. Under these conditions, the resultant grain size in the extruded workpiece would be 26 μ m, as determined in *CASE 1*. The extrusion was interrupted when the billet had only partially extruded through the die. The billet was subsequently removed from the tooling and water quenched. Between the end of extrusion and the beginning of quench 39 seconds elapsed.

The partially extruded billet was sectioned along a diametral plane and prepared for metallographic examination. The specimen was etched with 2% Nital to reveal grain boundaries for grain size

measurements. The grain sizes at different locations along the center-line of the workpiece in the deformation zone were measured using the Heyn intercept method [16]. The observed grain size was the result of dynamic recrystallization during extrusion and any grain growth that may have occurred during the 39 second transfer time. Figure 12 shows typical microstructures from the partially extruded billet. The experimentally measured grain sizes are shown in Figure 13. Clearly, the measured grain size was larger than the predicted grain size of 26 μ m. Therefore, an attempt was made to take into account any grain growth that may have occurred during the transfer time.

$$d^2 = d_0^2 + At \exp\left(\frac{-Q_{gg}}{RT}\right) \quad (17)$$

This extrusion experiment was simulated using the finite element simulation program ANTARES [17]. The billet and die domains were discretized to an average mesh size of 3 mm square. The finite element simulation was performed using an individual step increment approximately equal to 1/100 of the total ram stroke. The process was simulated for the nonlinear coupled response of the billet and the thermal response of the die. After the partial extrusion, the temperature at the billet centerline increased to 1313K due to deformation heating. The cooling of the partially extruded billet for 39 seconds was then simulated. Figure 14 shows the resultant evolution in temperature along the billet centerline. Based on this evolution of temperature and the experimentally measured grain size, the grain size variation along the billet centerline was calculated using the equation [14] where d_0 is the initial grain size, $A=1.44 \times 10^{12}$ (μ m)²/s, and $Q_{gg}/R = 32100$ K in the temperature range of 1050-1300K. The grain size variation along the centerline of the workpiece in the deformation zone, after the correction for grain growth, is also presented in Figure 13. As seen in the figure, the corrected grain size is very close to the desired value of 26 μ m.

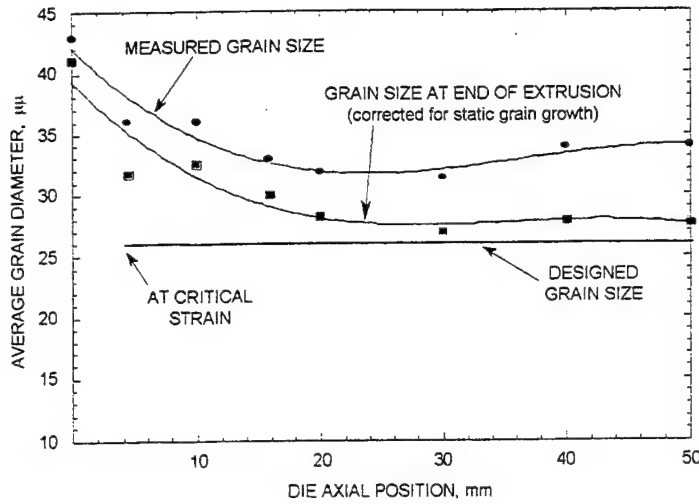


Figure 13. Measured and Corrected Prior-Austenite Grain Size Versus Position Along Die Centerline

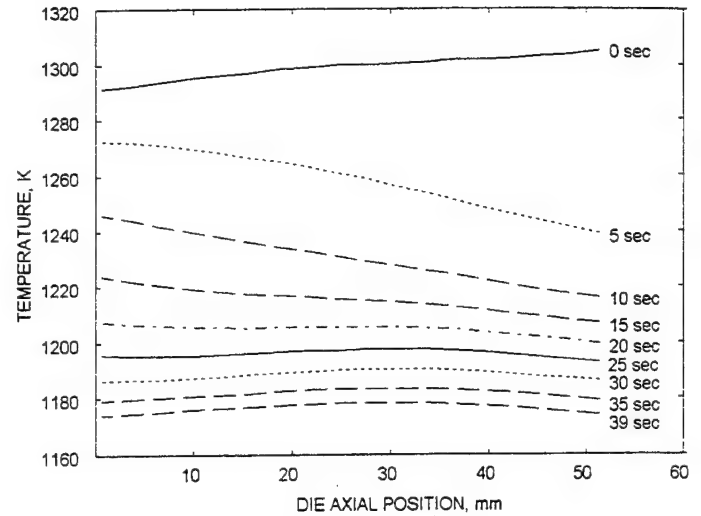


Figure 14. Simulated Temperature Distribution Along Die Centerline During Air Cooling Period

4.2.11 Summary and Conclusions

A two stage approach for optimal design of metal forming processes has been presented. The first stage involves determining an optimal material deformation path based on models for microstructural development, and the second stage involves determining the optimal process parameters that will impose the desired deformation path on selected areas of a workpiece.

The development uses equations developed by Yada et al. [13, 14] for dynamic recrystallization of plain carbon steel for the first stage to obtain an optimal material deformation path such that the

final grain size is maintained at 26 μm . This trajectory determination was performed via minimization of a cost function which included costs related to both final states and the trajectory followed by the material during processing. In the second stage, a geometric mapping was utilized to develop an extrusion die profile that would deliver the optimal trajectory computed in the first stage. This methodology suggests that using the same die shape, the grain size can be controlled through changes in initial billet temperature and ram velocity for the round to round extrusion case.

A validation experiment was performed by utilizing the extrusion die geometry obtained in the second stage. After correction for static grain growth, the grain size variation within the deformation zone of a partially extruded billet was found to agree with the desired grain size.

4.3 MODELING AND SIMULATION OF METAL FORMING EQUIPMENT

4.3.1 Introduction

The motivation for developing accurate models and computer simulations of metal forming equipment is three-fold. Firstly, the ability to quickly develop improved press control algorithms is greatly enhanced by the ability to perform repeated computer experiments without the need for costly and time-consuming experimental tests that can interfere with production. Secondly, as the use of finite-element modeling (FEM) techniques for the analysis and design of metalforming processes continues to increase and become more sophisticated, the need to integrate accurate

equipment models into the FEM-based simulations will increase. Thirdly, with the possibility of sensing workpiece conditions directly during forming operations (Mullins and Irwin, 1996) it is possible that in the future these measurements could be fed back to the metalforming equipment's control computer for control of the forming equipment in order to achieve final workpiece qualities even in the presence of variations in initial workpiece and equipment conditions. From a process control perspective, this approach should provide for the highest level of robustness and repeatability in production. Behind each of these motivational components is the need for improved control and predictability of the equipment's behavior. This need is driven by the desire to achieve near-net shapes, higher quality, higher yields, and better control of microstructure for parts made from hard-to-form materials.

4.3.2 Press System Description

A simplified block diagram of a typical hydraulic press system is given in Figure 15, where the lines represent possible directions of fluid flow. The system is powered by an electric motor that drives a hydraulic pump. Transient demands for high ram speeds are met by an accumulator system. A counter-balance is employed to support and return the main ram to the top of its stroke after a forging operation is completed. The servo manifold controls the flow of fluid to the main ram cylinder and to the tank.

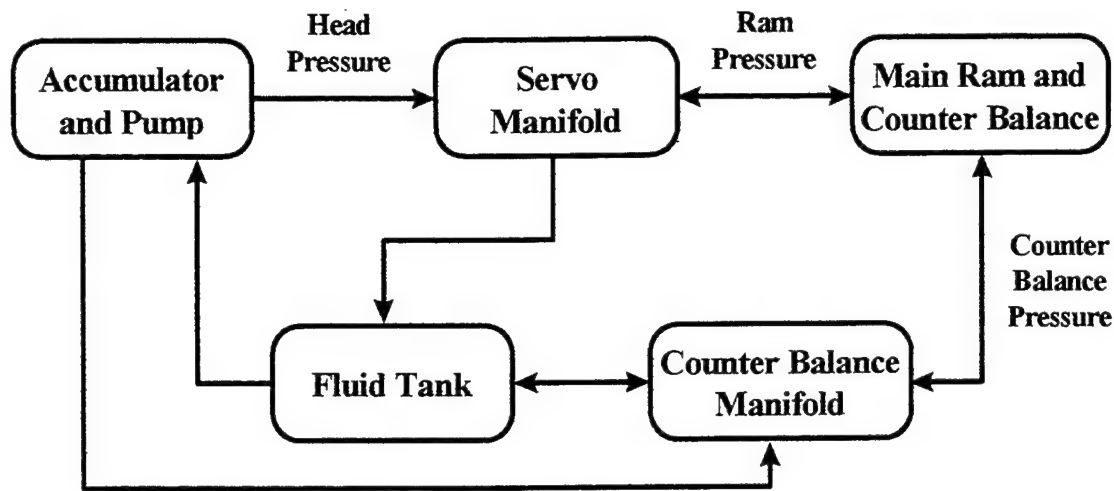


Figure 15. Simulated Block Diagram of a Typical Hydraulic Press

4.3.2.1 Hydraulics

The primary considerations involved in the modeling of hydraulics in a press system include the bulk modulus of the fluid, the flow rate of fluid from the pump, the head pressure, the flow rate through the servo manifold, and the main ram pressure. Other items that must be included are the hydraulic pressure on the counter-balance subsystem and pressure losses due to the flow of fluid through circular pipe.

4.3.2.1.1 Pumps. Most often pumps are driven at a constant speed by an electric motor while the amount of fluid being delivered by the pump at any moment is usually governed by the position of an actuating spool of a servovalve^[1]. The time response of this servovalve is the dominant factor in the dynamic performance of the pump. Therefore, from a *mechanical response*

perspective, the modeling of pump behavior can be viewed as being similar to the mechanical response of servovalves in general as will be discussed in section 4.3.2.2.

4.3.2.1.2 Head Pressure. The head pressure of a pump-only system or a system using an accumulator in which the separator tank is completely full or empty is modeled from first principles of fluid mechanics [1] by the relationship

$$\dot{P}_{head}(t) = \frac{q_{pump}(t) - q_{sm}(t)}{C_{head}(t)}, \quad (18)$$

where q_{pump} , q_{sm} and C_{head} are the volumetric flow rate into the volume between the pump and the servo manifold, flow rate out, and hydraulic capacitance of that volume, respectively. The hydraulic capacitance is simply

$$C_{head}(t) = \frac{V_{head}(t)}{\beta} \quad (19)$$

where V_{head} and β are the volume between the pump and the servo manifold and the bulk modulus of the fluid, respectively. The volume is shown to possess a time dependence to account for the fact that the volume can change if there is an accumulator in the pump circuit. In systems employing accumulators in which the separator tank is not full (the usual case), the head pressure is given by

the differential equation

$$\dot{P}_{head}(t) = -\frac{P_0 V_0}{V_{nit}^2(t)} \dot{V}_{nit}(t), \quad (20)$$

where P_0 , V_0 , and V_{nit} are initial head pressure, initial volume of nitrogen, and instantaneous volume of nitrogen, respectively. Assuming the hydraulic fluid is incompressible with respect to the nitrogen, the instantaneous volume of nitrogen is determined from the net flow of hydraulic fluid into the head volume, i.e.,

$$\dot{V}_{nit}(t) = q_{pump}(t) - q_{sm}(t). \quad (21)$$

4.3.2.1.3 Ram Pressure. The most important hydraulic component affecting ram speed is the pressure on the ram piston. This pressure is modeled by the differential equation

$$\dot{P}_{ram}(t) = \frac{q_{sm}(t) - A_{ram} v_{ram}(t)}{C_{ram}(t)}, \quad (22)$$

where A_{ram} , v_{ram} , and C_{ram} are the cross-section of the ram piston, velocity of the ram and hydraulic capacitance of the fluid volume between the servo manifold and the ram piston, respectively. This capacitance is given by

$$C_{ram}(t) = \frac{V_{nom} + A_{ram} \Delta x_{ram}(t)}{\beta}, \quad (23)$$

where V_{nom} and Δx_{ram} are the nominal volume and the displacement of the ram from its nominal position, respectively. The term $A_{ram}v_{ram}(t)$ located in the numerator of Equation 6 takes into account the effect of the rate of change of the volume as the ram descends. The force applied to the main ram due to the ram pressure is $F_{sm}(t) = P_{ram}(t)A_{ram}$.

4.3.2.1.4 Counter-balance Pressure. The counter-balance pressure in press systems is commonly maintained by a relief valve. The relief pressure of this valve is chosen so that the weight of the ram can be supported entirely by the counter-balance cylinders. The weight that can be supported by such a system is given by

$$W_{sup} = A_{cb}P_{rv}, \quad (24)$$

where A_{cb} and P_{rv} are the cross sectional area of the counter-balance pistons and the relief valve pressure, respectively. When pressure is applied to the ram by fluid from the servo manifold, the load on the counter-balance exceeds W_{sup} and the relief valve opens allowing fluid to flow and the ram to descend. The force (no load) applied to the ram via the counter-balance is given by

$$F_{cb}(t) = A_{cb}P_{rv} + \gamma_{cb}A_{cb}\dot{x}_{ram}(t), \quad (25)$$

where the term $\gamma_{cb} A_{cb} \dot{x}_{ram}$ represents the additional force applied to the ram due to the frictional effect of fluid flowing through pipe. The parameter γ_{cb} is a factor for determining the frictional force per unit of volumetric flow rate. It is determined from the Hagen-Poiseuille Law [2] :

$$\gamma_{cb} = \frac{128\mu L}{\pi D^4} \quad (26)$$

where D and L are the diameter and length of the pipe in inches, and μ is the viscosity of the fluid.

This effect can add a significant amount of viscous damping to the overall system.

4.3.2.2 Servovalves

The primary factors determining the flow of fluid through the servo manifold are the current state of the servovalve and the differential pressure across the valves. Although higher-order nonlinear analytical models of the mechanical behavior of servovalves can be developed from first principles, second or third-order linear models identified from experimental data have proven to be quite satisfactory for producing accurate simulations. A typical model in state-variable form [5] is given by

$$\begin{aligned} \dot{x}_1(t) &= x_2(t) \\ \dot{x}_2(t) &= A\omega_n^2 v(t) - 2\zeta\omega_n x_2(t) - \omega_n^2 x_1(t) \end{aligned} \quad (27)$$

where x_1 , x_2 , and v are the spool position, spool velocity, and applied voltage, respectively.

A , ω_n , and ζ are the gain (e.g., in./volt), natural frequency and damping ratio of the valve.

Equation 10 only describes the mechanical response of the power spool. The volumetric flow rate of fluid through a three-way servovalve into the main ram fluid volume can be modeled as a

$$q = \text{sgn}[x_1(t)] \text{sgn}[\Delta P(t)] f[|x_1(t)|] \sqrt{|\Delta P(t)|} \quad (28)$$

where

$$\Delta P(t) = P_{head}(t) - P_{ram}(t) \quad (29)$$

function of the position of the power spool and the differential pressure across the valve by a modified orifice flow equation [1] and the function f is an experimentally determined relationship between spool position and flow rate. Experience reveals that a third degree polynomial is usually sufficient for the function f . Typical flow curves for a servovalve are shown in Figure 16. for several values of differential pressure. The use of the signum function provides a means for modeling the flow direction switching capabilities of a three-way valve. The four flow possibilities are defined in Table II.

Table II. Flow Possibilities for a Three-way Servovalve

	$\Delta P < 0$	$\Delta P \geq 0$
$x_1 \leq 0$	Tank to Ram	Ram to Tank
$x_1 > 0$	Ram to Head	Head to Ram

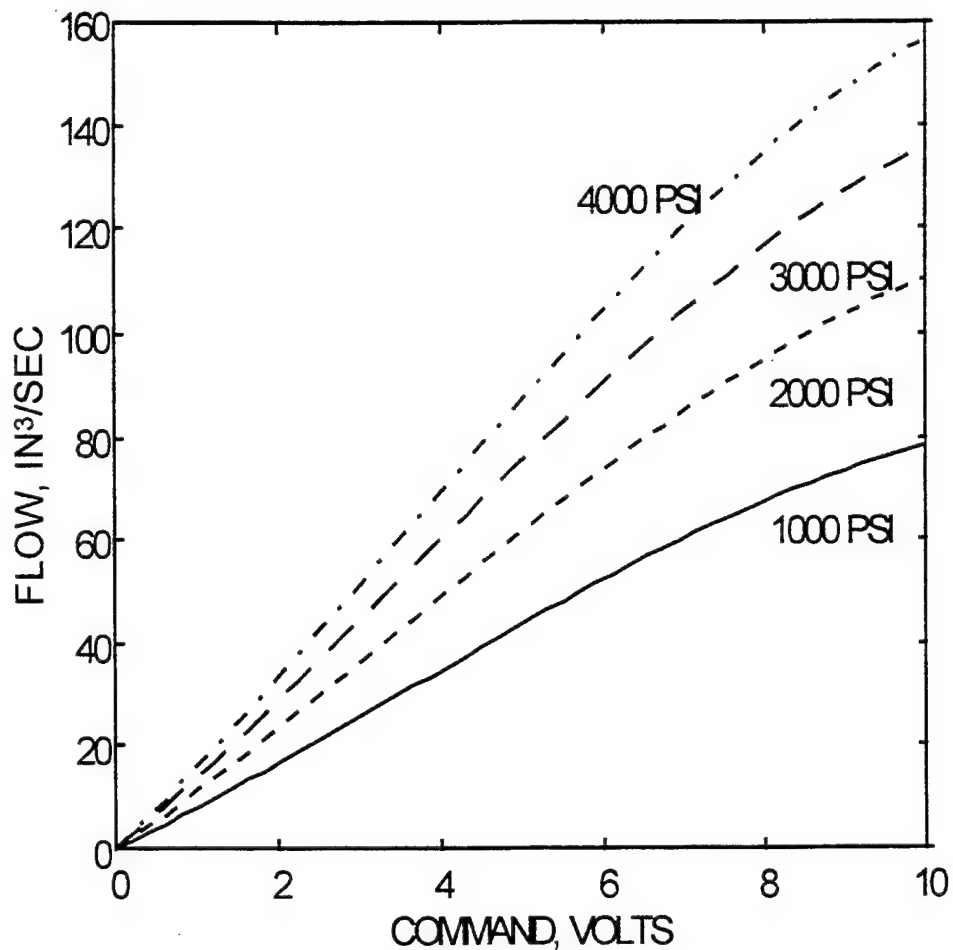


Figure 16. Typical Flow Curve for a Servovalve as a Function of Spool Position

4.3.2.3 Ram Dynamics

The ram can be modeled as a rigid body with a mass M possessing a single degree of freedom. More complex bending and inertial effects can be included if increased precision is justified. The equation of motion for the ram is given by

$$a_{ram}(t) = [F_{sm}(t) - F_{cb}(t) + W_{ram} - F_{fric}(t) - F_{load}(t)] / M_{ram} \quad (30)$$

a_{ram} = acceleration of the ram

F_{sm} = forces due to hydraulic pressure from servo manifold

F_{cb} = forces due to hydraulic pressure from counter-balance

W_{ram} = weight of the ram

F_{fric} = frictional forces

F_{load} = forces due to workpiece loading

M_{ram} = mass of the ram.

The force of friction F_{fric} between the ram piston and the seals can be modeled as coulomb

friction [7]. Values for the parameters associated with this difficult-to-measure effect are best determined by adjusting the simulation parameters to best match the experimental data. A model for this effect is given by

$$F_{fric}(t) = \text{sgn}(v(t)) * [c|v(t)| + b] \quad (30)$$

where $v(t)$ is ram velocity, c is similar to the effect of viscous friction and b is an offset that models the effect of sticking. Note that if b is zero, then this model reduces to the standard model of viscous friction. The accurate modeling of the workpiece loading F_{load} is very difficult for situations involving the forming of complex shapes due to the interaction of the workpiece and dies

and the mechanical properties of the workpiece material. In most instances it is necessary to make simplifying assumptions in order to formulate a practical model.

4.3.2.4 Sensors

A modern press system can employ several types of sensors for safety, diagnostics, and feedback control. For the purpose of feedback control, measurement of pressure, linear displacement and linear velocity are most important. The pressure transducers [3] are employed to measure the head pressure and the pressure on the ram piston. Since the difference in these pressures provides for the differential pressure across the servo manifold, the control computer can use this difference for determining commands to the servovalves. This is the most common method employed for ram speed control. Used alone, it has the disadvantage of requiring very accurate models of the flow curves of the servovalves since the actual ram velocity is not actually used. Any error in the flow curve models will translate directly into errors in ram speed. The measurement from the head pressure transducer is also useful for actuating the main pump in order to maintain the appropriate head pressure. The response time of a pressure transducer is significantly shorter than that of a press and therefore these transducers and their associated electronics can safely be modeled as simple gains, i.e.,

$$\text{Voltage} = \text{Gain} * \text{Pressure.} \quad (32)$$

Linear displacement transducers [4] play a critical role in measurement of ram stroke. High accuracy and precision of these sensors is very important for ensuring repeated part quality. Various types of linear displacement transducers are available that use a variety of technologies. Most of these have very rapid response times and can, like pressure transducers, be modeled as simple gains. Direct measurement of ram velocity is very difficult due to the lack of availability of reliable sensors for measuring translational velocity over a large dynamic range. A common method employed for obtaining translational velocity estimates is to numerically differentiate successive position measurements. This method is fraught with pitfalls and must be used with extreme caution due to the presence of electronic and analog-to-digital converter quantization noise [6] on the position measurements. The quantization noise problem is especially acute in situations where low velocities and high computer sampling rates are present. The simplest velocity estimate is calculated by

$$\hat{v}(t) = \frac{s(t) - s(t - T)}{T} \quad (33)$$

where T is the sampling period and s is ram position. More complex schemes can be employed that are effectively digitally filtered estimates of velocity [6]. These techniques reduce the effect of noise problems at the expense of reducing response time. In many applications this trade-off is justified. Another method that can be employed is to numerically integrate accelerometer measurements. This technique considerably reduces the noise problem, but can introduce errors due to drift in the

accelerometer output. The formula for the trapezoidal integrator is given by

$$\hat{v}(t) = \hat{v}(t-T) + \frac{T}{2} [a(t) + a(t-T)] \quad (34)$$

where a is ram acceleration.

4.3.2.5 Control Processor

Press systems typically use two levels of processing for control. The highest level of control is usually called a supervisor and provides functions such as engaging safety locks, monitoring pressure switches for excessive pressures, etc. This level of control is usually provided by an industrial programmable logic controller (PLC). The lower level of control is usually called the servo loop and is responsible for having the main ram track the desired velocity or position profile. This level of control can be provided by a PLC with special servo control features or by a industrial PC-based system with custom software. Input to and output from the computer control system is usually provided by 12-bit analog-to-digital (A/D) and digital-to-analog (D/A) converters, respectively. Modern electronic computer control systems have the capability of providing very high sampling rates which provide in theory the capability of rapid response to changes in load conditions. However, the use of excessively high sampling rates can introduce problems as described previously.

4.3.3 Computer Simulation of Dynamic Systems

The use of a system model to predict the behavior of an actual system is desirable in many situations. In the case of design, the actual system may not yet exist and it may be desired to evaluate several possible configurations. In the case of analysis, an experiment on the actual system may take too much time or too little time, may be too expensive, or may even destroy the system - very likely an undesirable situation. Many complex, real-world systems cannot be accurately described by mathematical models that can be evaluated analytically to obtain responses to particular set of inputs or parameters. The simulation alternative consists of evaluating the model numerically with the inputs and parameters in question to determine how the outputs of interest are affected [8].

Simulation has been a tool for analysis and design of engineering systems for many years now. In particular, simulation of continuous time and discrete time dynamic systems has been the subject of vast research for several decades. Simulation languages such as CSMP™ and ACSL™ have been specifically developed for building dynamic system simulation models.

4.3.3.1 Graphical Simulation Paradigm

The state of the art in simulation of dynamic systems includes software packages that not only aid the engineer in building simulation models, but facilitate the creation of models and interpretation of

results by means of sophisticated graphical user interfaces. Simulink™, VisSim™, and Matrix™ are three of the several packages of this nature that are available.

In the sense used here, a simulation model is represented by a block diagram in which all relevant elements and relationships that model the system are included. For the case of the forging system under consideration, which includes the forge press, the workpiece loading, and the internal mechanisms by which the microstructure of the workpiece evolves, the top level block diagram of a Vissim™ simulation model is shown, for illustration purposes, in Figure 17. Each block in such a simulation diagram models an element or group of elements in the actual system, a data input port, or an output port. Each line represents a path for the flow of information or energy. Note in Figure 17, that the fundamental blocks in the forging process simulation are the forge press, the controller, and the tooling package. Each of these blocks is comprised of several levels of subsystems, which can be observed with convenient editing tools in the graphical simulation environment.

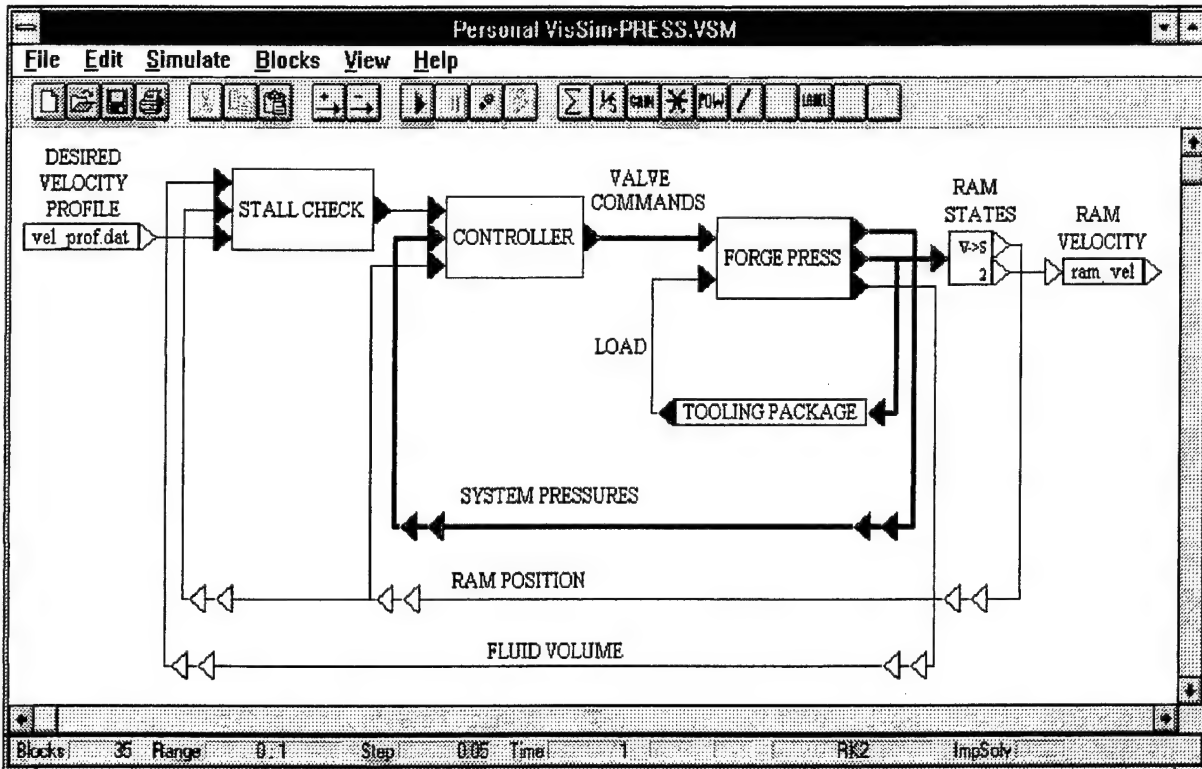


Figure 17. Vissim™ WINDOW, Top Level Diagram of a Forging Process Simulation

4.3.3.2 Automatic Equipment Simulation Code Generation for the Metal Forming Industry

One objective underlying this work is to provide the metal forming industry with scientifically based tools that will expedite design by allowing the user to perform what-if studies that include all aspects of the manufacturing process. For that reason, it is desired to provide the user with a software module that will generate the response of the system to specific inputs without having to use a simulation package; i.e., a standalone program or a set of routines that will simulate the system without the need for a dedicated simulation software package on the part of the end user.

This can be achieved by using automatic code generation features that can be purchased for any of the state-of-the-art simulation packages mentioned above.

The idea here is to build the simulation model in one of the available simulation software packages and then generate high level language code that can be compiled to generate a program or library that will simulate the system. The original simulation model can be developed by a consulting firm that can deliver executable code or libraries for the simulation of the particular system. Such executable or library can then be used in conjunction with existing finite element analysis software for the simulation of the forging process by the engineer in charge of the design.

4.3.4 Application to the Erie 1000 ton Forge Press

The Erie 1000 ton forge press located at Wright-Patterson Air Force Base (WPAFB) is a vertical hydraulic forge press possessing a programmable, computer-based ram velocity control system employing hydraulic pressure and ram position feedback. The press was manufactured by Erie Corporation, Erie, Pennsylvania, while the hydraulic control system was designed and built by Oilgear Inc., Milwaukee, Wisconsin. The press has been in service since 1992 for performing manufacturing and metallurgical research at WPAFB. The power plant consists of an axial piston pump with 82 gallons per minute (gpm) capacity driven at 1200 rpm by an 200 hp electric motor. Transient demands for higher flow rates are provided by a 16 gallon hydraulic separator tank and 195 gallon nitrogen bottle. Nominal head pressure is 3800 psi. The stroke of the ram is 15 inches and the maximum speed of the ram is approximately 300 in./min. This maximum speed cannot be

maintained over the entire stroke due to the limited capacity of the pump and size of the separator tank. The cross sectional area of the main ram piston is 591 inches. The main ram is supported by two counter-balance pistons with cross sectional areas of 28.86 inches each. The relief valve pressure on the counter-balance is 1000 psi. This implies that the counter-balance can support 28.86 tons. The nominal weight of the main ram is 21 tons.

The speed of the press is regulated by the use of two Oilgear three-way servovalves and one Parker proportional throttle valve. The gains of these valves are:

Oilgear 800 three-way servovalve	6 (gal/min)/volt @ 3000 psi
Oilgear 1600 three-way servovalve	36.7 (gal/min)/volt @ 3000 psi
Parker TDA 100 proportional throttle valve	330 (gal/min)/volt @ 3000 psi

The use of these three valves in parallel provides capability for wide dynamic range and precise control of ram velocity. The valves are controlled by an Intel 80368-based industrial computer that uses head pressure, ram pressure and ram displacement feedback for control of velocity. The details of the Oilgear-developed control law for the valves are proprietary and cannot be provided.

4.3.5 Erie Press Simulation

Using the principles described in Section 4.3.2, a computer simulation was developed using the simulation software SIMULINK™. The block diagram for the overall press system is shown in Figure 18. This diagram shows the interconnections between the forge press, the control computer,

67

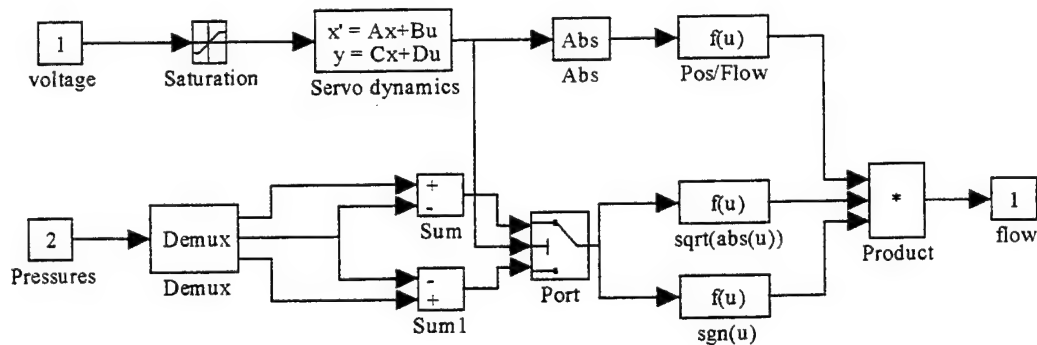


Figure 20. Three-way Servovalve Block Diagram

In order to verify that the computer model is accurate, experimental data from a simple forging was recorded and compared with the corresponding simulation data. The experimental forging was a cylindrical upsetting of steel. The press was programmed to forge at a constant velocity of 30 in/min. Plots of the experimental and simulated ram velocity and position are shown in Figure 21 and Figure 22, respectively. The irregularity in the experimental data of Figure 21 is due to the method used by the press' computer to estimate the velocity. This behavior is not present in the actual press motion. Other than this effect, the simulation data is seen to closely resemble the experimental data. The data clearly reveals the ramping up and overshoot of the desired velocity. The brief change in velocity due to impact with the workpiece is clearly observed near 3.5 seconds.

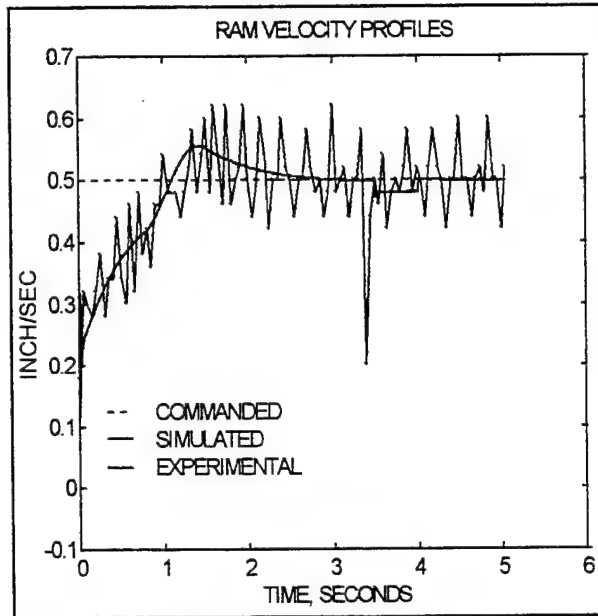


Figure 21. Plots of Experimental and Simulated Ram Velocities

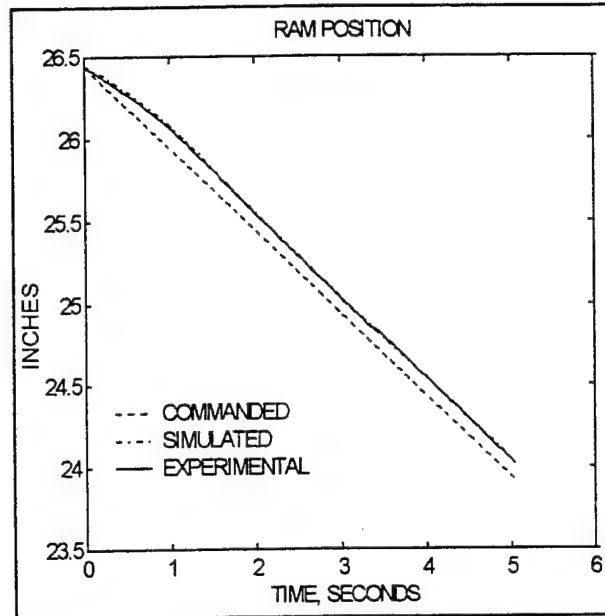


Figure 22. Plots of Experimental and Simulated Ram Position

Figure 23 shows the experimental and simulated results for the ram load as derived from the ram pressure measurement. The plot reveals that approximately 10 tons are

needed to overcome the counter-balance and frictional forces. The load increases rapidly beginning at approximately 3.5 seconds.

This corresponds to impact with the workpiece. Beginning at approximately 4 seconds, elastic deformation of the workpiece and tooling ceases and plastic deformation of the workpiece begins. It is clear from the data

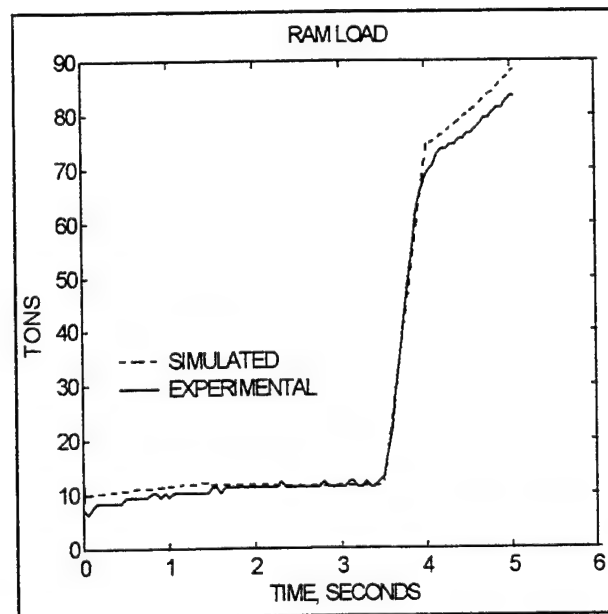


Figure 23. Plots of Experimental and Simulated Ram Load

that the press was able to maintain the desired velocity under load, as long as the load was not increasing too rapidly.

The press' computer does not record the commands to the hydraulic valves, but it is interesting to observe the plots of these commands and the corresponding valve flows from the simulation. These plots are shown in Figures 24 and 25, respectively. Notice that a particular valve command does not always result in the same flow rate. This is due to the changing pressure across the servo manifold. Figure 25 clearly reveals that flow can decrease even as the command increases.

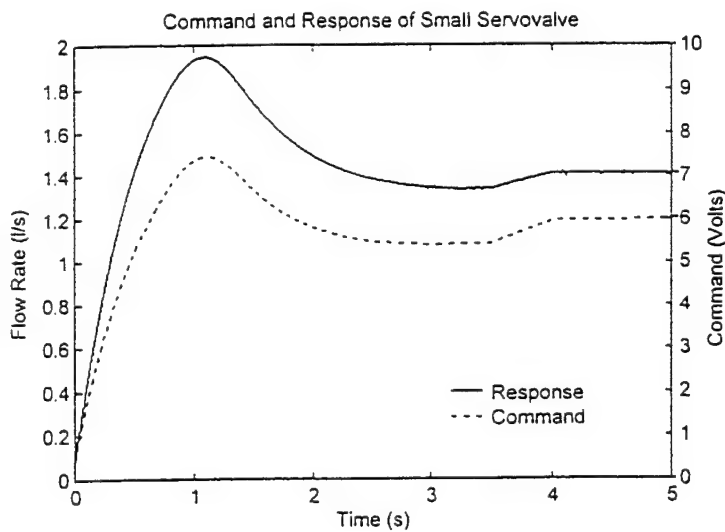


Figure 24. Simulation results for small servovalve command and response

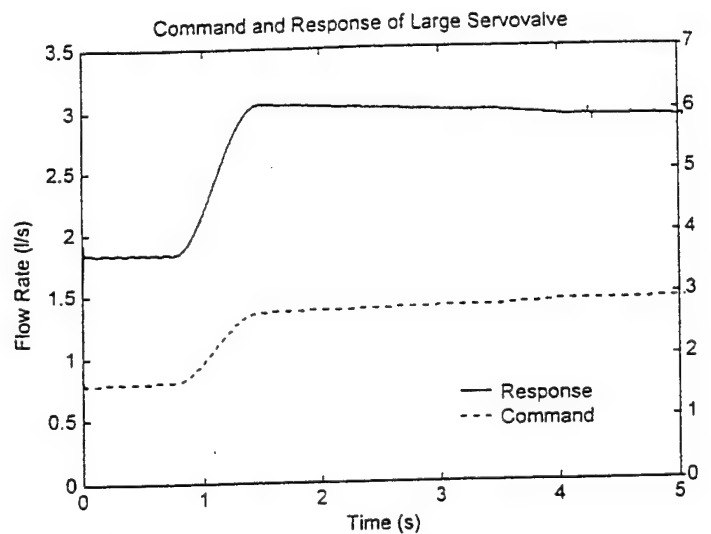


Figure 25. Simulation results for large servovalve command and response

4.3.6 Conclusions

The use of graphics-based system modeling and simulation software greatly assists in making the modeling process systematic, self-documenting, accurate, and time efficient. The ability to quickly perform "what if" experiments with regards to different control strategies, sensors, actuators, and tooling aids the engineer in making informed decisions regarding potential changes to existing metal-forming equipment and/or processing operations. For example, this approach makes it possible for the engineer to answer questions concerning the wisdom of possibly adding a sensor for direct measurement of ram velocity for feedback control of the ram velocity as opposed to simply using pressure feedback. As the need for precise control of ram velocity, as well as position, increases, the need for direct measurement of velocity as a feedback control signal will become more acute. Current techniques for controlling velocity (inversion of servovalve flow models combined with pressure measurements and numerical differentiation of displacement measurements) are not adequate for high performance.

Experience has revealed the need for press operators to customize the press control law in order to achieve the desired velocity profile for different forming operations. Having a custom control law for equipment that repeatedly makes the same part for several weeks or more is satisfactory, but as the need to use the same equipment for several different parts in a day or custom small lots increases, having to repeatedly tune the control law can waste a significant amount of time. Control laws need to be designed to be robust so that different loading conditions and velocity profiles can be handled successfully without the need for customization.

It is anticipated that future work will include the use of the automatic code generation features of modern simulation packages to integrate accurate equipment models into finite-element simulation software in order to further improve the accuracy of computer simulation of metalforming processes.

4.4 PRECISION DIE DESIGN

4.4.1 Introduction

The controlling driver in manufacturing is cost reduction for all components used to fabricate structures. The focus on component manufacturing cost reduction will contribute significantly to the reduction of acquisition costs for new products. This is called affordability, whether the parts are for the military or commercial markets. An aggressive goal for cost reduction brings into focus the relative processing requirements and the cost performance of candidate high strength material product forms used by OEM's, subcontractors and machining sources in component manufacturing streams.

Precision forged parts, in general, are a preferred raw material product, since forgings have superior mechanical properties and other product performance attributes. Closed-die forgings are a preferred product also, because they have the potential for reducing the consumption of energy. Forgings in netshape form sometimes encounter machining distortions due to quenched in residual

stress patterns, and, therefore, it is essential to understand each step of the forging realization process. Designing a machining-friendly forging requires the product and process designers to work together in a concurrent engineering mode, as many tradeoffs may be required between product requirements, die and preform design, process control, quality assurance, heat treatment and machining to achieve an affordable and design acceptable part. The geometrical attributes of netshape forged parts must be balanced to achieve satisfactory functional performance, machining performance and die life.

The goal is to reduce significantly the cost of manufacturing netshape forgings. To make netshape forgings universally affordable, new engineering and manufacturing capabilities must be developed. The following enumerate lists some of the requirements for affordability and cost reduction.

New Engineering & Manufacturing Capabilities

- Design Tools, Models and Simulations to Optimize Products & Processes and Make an Error Free Transition to Production.
- Forging Systems that Decouple Cost From Quantity & Make Rapid Commercial Changeover.
- Enterprise-wide CAD/CAM/CAE to Reduce Overheads & Improve Program Control.

The new engineering and manufacturing capabilities enumerated above should address three fundamental priorities of the military and industry. These requirements are cost, performance and

schedule. These priorities focus on reducing the netshape part development time and economic order quantities (EOQ's) of parts.

4.4.2 Forging Design Rules for Quality Assurance

Quality assurance requirements for forging design and production can be divided into two areas of dimensional and material control. Dimensional control is concerned with the effects of shrinkage, die wear, residual stress and die closure variations during forging production runs. *The effects, which these design variables have on cross-sectional areas to achieve the required mechanical properties, is the primary focus of design for dimensional control.* Material control activities include ultrasonic, die penetrant and magnetic particle inspection. Both material and quality control areas should be considered concurrently during forging design, and these considerations must be maintained throughout production of the netshape forging to ensure a consistent and reliable finished product. The Forging Die Design Sequence is shown in Figure 26.

4.4.2.1 Dimensional Control

Dimensional control of netshape structural forgings is necessary to ensure the following design objectives:

- Each forging will yield the machined parts for which they were designed.

- The forging does not become too large to cause excessive machining.
- The forging does not become too large and causes an increase in the starting stock size used to make the forging.
- Oversize cross-sections do not adversely affect the forging's mechanical properties.
- Netshape forgings that require no surface machining meet "Fit and Function" requirements and their installed weights are controlled.

4.4.2.2 Forging Envelope

A forging outline is built up by making material allowances for the forging and adding them to the basic machine part geometry. Figure 27 is a combined cross section of a forging and machining, which shows how allowances for the forging tolerances are applied. The material allowances that produce the Forging Envelope Requirements are listed in Figure 28.

The significant features shown in Figure 27 are the Machining (.06") and the Tooling (.03"). These provisions ensure that enough material remains, even if the forging tolerances are simultaneously at their worst conditions, .09" per surface, to allow 100% machining cleanup. The .09" allowance has additional value, because it allows near and far surface resolution problems during ultrasonic inspection.

The forging dimensions and tolerances, and the locations (datum planes) from which they originate are carefully considered to provide the lightest weight forging and best overall quality control. *The primary tolerances which control*

the forging features and cross-sectional areas are the shrink variation, die wear (DW), Die Closure (DC), Straightness and Mismatch.

Forging Envelope Requirements

- Negative Die Closure Allowance
- Machining Allowance
- Tooling Allowance
- Straightness Allowance
- Mismatch Allowance
- Shrink Allowance
- NDI Allowance

Figure 28. Allowances for Forging Tolerances

Shrinkage Variation — Shrinkage variation is the allowable variation in the length and width dimensions of the forging after it is removed from the die and cools to room temperature. This variation is a function of the coefficients of expansion of the workpiece and die block, and their respective temperatures when the forging is struck.

Forging datum planes are established in the length and width directions from which material shrinkage variations are calculated. *An allowance to compensate for the shrinkage variation is*

added to each surface controlled by a length and width dimension. The effects of shrinkage and material added for compensation increase with distance from the datum planes. Placement of the datum planes relative to the part geometry is an important consideration when attempting to produce a minimum weight forging. On large forgings ($> 50''$), the datum planes are usually positioned within the part geometry and weighted toward the wider or more detailed end. Figure 29 illustrates this design concept. *This weighted datum reduces the amount of shrinkage stock allowances on part features, and it roughly divides the mass of the material into two equal parts.*

In contrast, shrinkage variation buildup is not as significant in small forgings. Thus, for ease in preparation of machine tools and fixtures, length and width features of a small forging ($< 50''$) can be dimensioned from a datum plane established at one end of the forging. The placement of datum planes for a small forging is shown in Figure 30.

Die Wear — Die wear occurs as a result of grinding and polishing of the die cavity to repair operational damage. This damage includes gouges and scratches caused by tools (tongs) used to remove the forging from the die, abrasion caused by material flow during forging, plus damage caused by scale and lubricant removal. In addition, the die sinker's tolerances are considered also as part

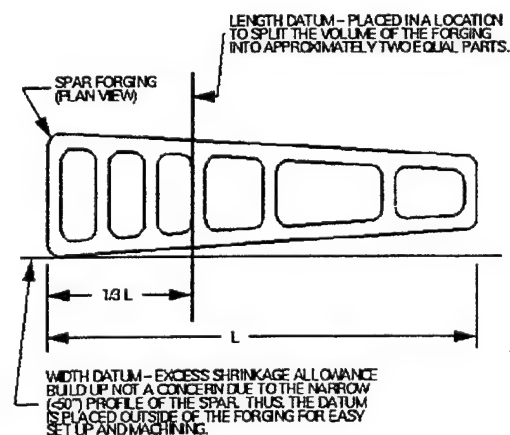


Figure 29. Typical Placement of Length and Width Datum Planes for a Spar Forging

of the die wear. Figure 31 details the features of a conventional die that are considered *high wear* areas.

It is not necessary to add an allowance for die wear to the forging envelope when designing the forging, since the machined part can always be obtained as the forging grows larger. However, the tolerances, which are applied to the length and width dimensions, must consider the die wear on each surface in addition to the shrinkage variation. *Figures 32 and 33 illustrate the application of the shrinkage variation (S), and die wear allowance (DW) in arriving at appropriate length and width tolerances.*

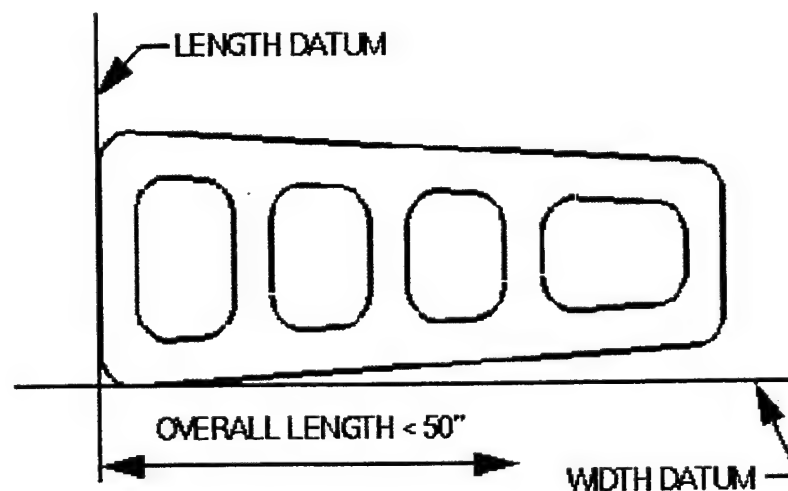


Figure 30. Typical Placement of Length and Width Datum Planes for a Small Forging

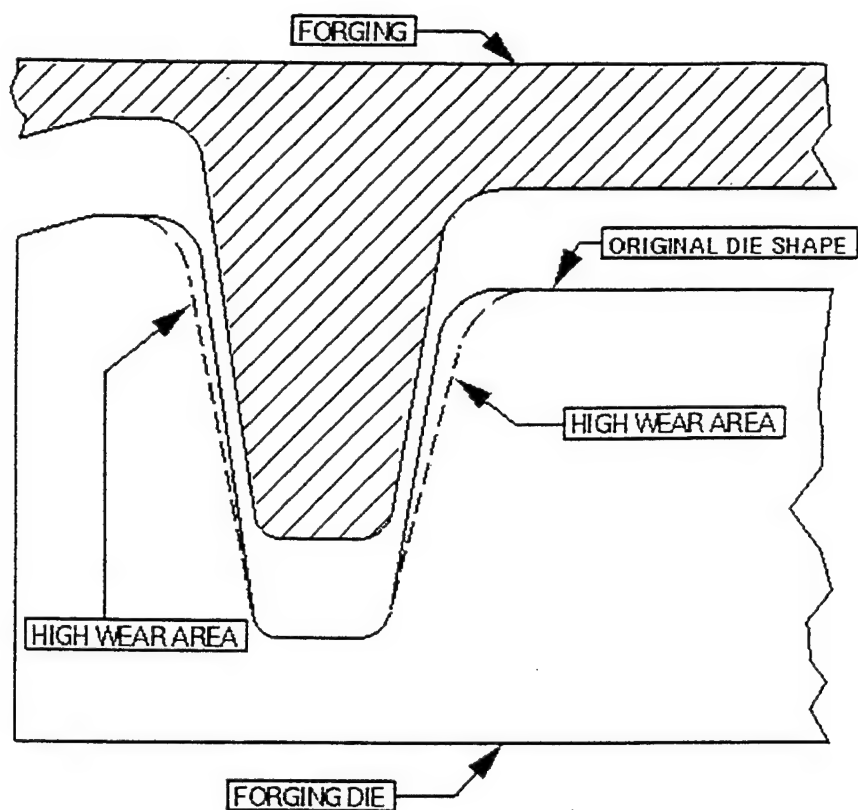


Figure 31. High Wear Areas for Forging Dies

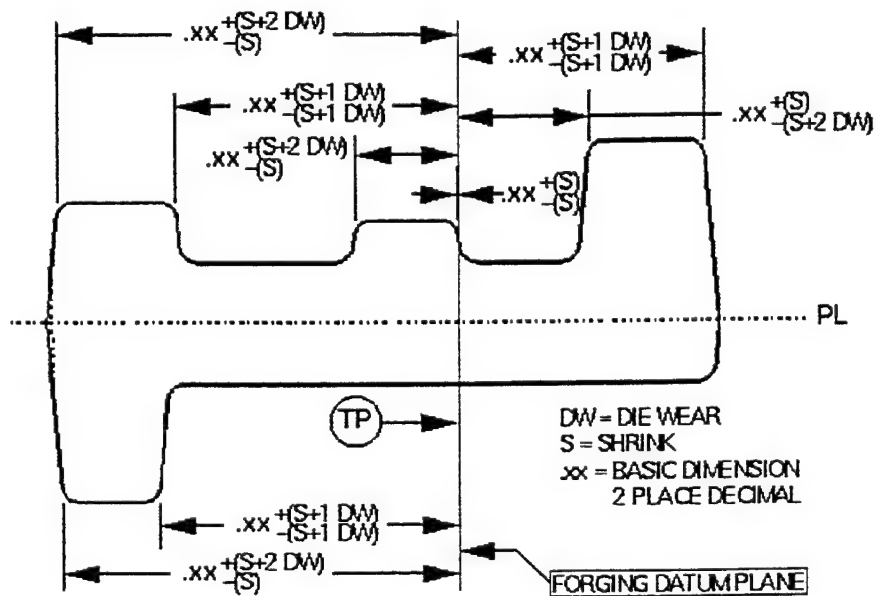


Figure 32. Shrinkage and Die Wear Tolerance Application for Large Forging with Datum Plane Inside Forging

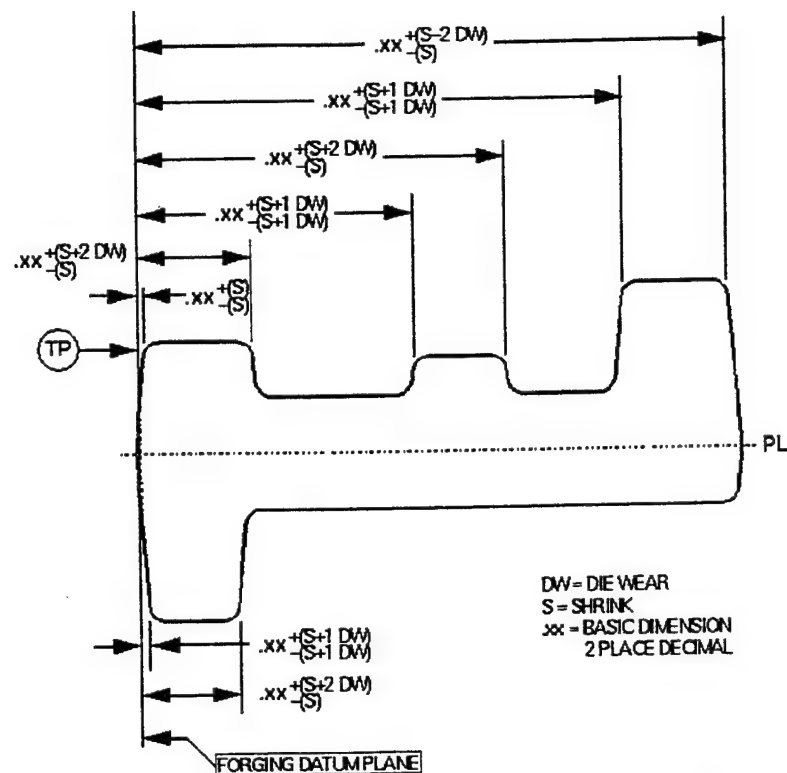


Figure 33. Shrinkage and Die Wear Tolerance Application for a Small Forging with Datum Plane on Periphery

Die Closure — Variations in the forging's thickness are possible, since the size and weight of the starting preform or billet are not constant. This variation is called die closure. The die closure tolerance is comprised of plus and minus (\pm) values. The latter (-) variation is of concern in assuring machining cleanup. Material is added in the forging envelope to dimensions that cross the parting line of the forging, such as ribs and webs tops, to compensate for the negative variations. In practice, an amount of material, equal to the magnitude of the negative die closure tolerance, is allowed on overall thickness dimensions. Half of the tolerance is allowed in each die half. The plus (+) die closure tolerance increases the envelop of the forging, and it is favorable in assuring machining cleanup. No stock allowance to the forging envelope is required for the plus die closure tolerance. Shrinkage variations and die wear tolerances are not additive to the die closure or thickness tolerance, which is shown in Figure 28.

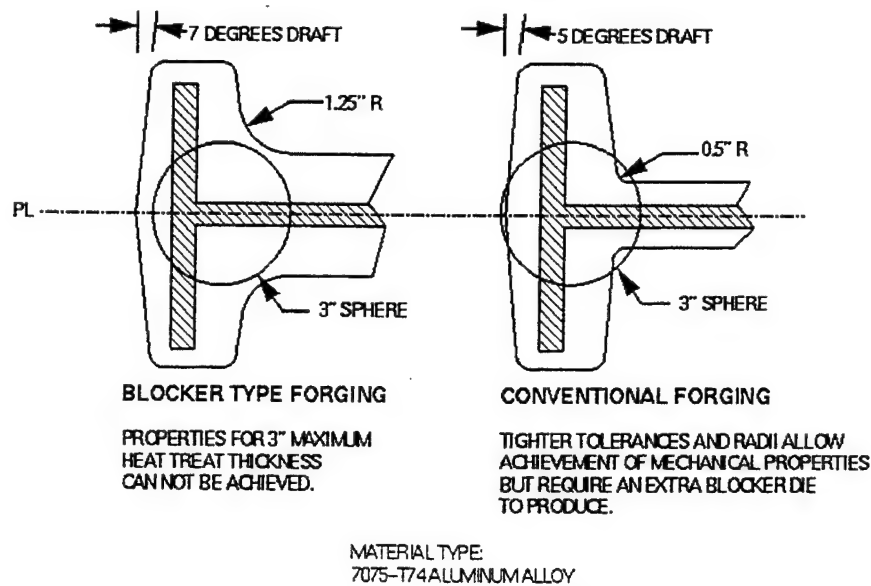


Figure 34. Comparison of Geometries to Achieve Mechanical Properties

Straightness and Mismatch — Allowances for these variables are included in the forging envelope buildup as shown in Figure 28. Once they are established in the forging envelope and the dies are sunk, they do not affect the forging size or weight during production. It is only necessary to check the production forgings to assure compliance to their established limits.

4.4.2.3 Design to Achieve Mechanical Properties

Cross-sectional area and localized masses affect mechanical properties, which metallurgists can obtain from the forging after heat treatment. To achieve the desired mechanical properties, it is sometimes necessary to design a more highly detailed, i.e., closer than normal, forging to reduce the mass and cross-sectional areas. A comparison of geometries to achieve mechanical properties is

illustrated in Figure 34. The increased definition may result in the need for an additional blocker die to produce the required shape. Table III shows the cross-sectional areas related to achieving material strength for a number of engineering alloys.

Table III Material Strength as a Function of Cross-sectional Area		
Material	Maximum Thickness (Inches)	Minimum Tensile Strength (Psi — Parallel to Grain)
Aluminum:		
7075-T74	3	66,000
7050-T746	6	70,000
7175-T746	6	68,000
061-T6	4	38,000
Titanium:		
Ti-6Al-4V	6	130,000
Stainless Steel:		
PH13-8Mo	12	205,000
Cond: H1000		

4.4.3 MATERIAL CONTROL

Material allowances are made during forging design to help control the soundness of the workpiece material throughout the entire production cycle. Three nondestructive inspection (NDI) methods are commonly used throughout the industry, and these methods are ultrasonic, die penetrant and magnetic particle inspection. The method or methods used and the level of inspection depends on the criticality of the part in service, its material type, and whether the part is used as-forged or

machined all over. Ultrasonic inspection detects internal flaws, while die penetrant and magnetic particle inspection techniques are used to find surface defects. The forging designer must add material allowances to the forging design to provide sufficient material for each of these NDI techniques to detect a flaw properly. This section briefly explains the rationale for making material allowances to accommodate the inspection methods.

Ultrasonic Inspection — Ultrasonic inspection is used to detect and estimate the size of internal flaws and discontinuities in the billet, preform and forging. The method uses a transducer that transmits ultrasonic sound waves into the test material and receives back reflections of any discontinuities. The inspection technique works for any class of engineering alloy, since only sound waves are involved. *Ultrasonic inspection has difficulty in detecting defects that lie on near and far surfaces.* This is an encumbrance of the method that must be worked around. The forging designer generally makes a material allowance to enable the forging to be inspected in a *rough* machined state. This forging state is shown in Figure 35. Figure 35 shows how this procedure isolates the actual machining within a *rough shell* of forging material. *Excess material* is left in the near and far surface problem areas to permit the entire machining to be inspected by the ultrasonic inspection method.

The part designer will determine the class and frequency of ultrasonic inspection beginning with the starting stock through forging and finished machining. The frequency of inspection is dependent upon the service load characteristics and operational criticality of the forged part. For fracture critical parts, which are life threatening, and maintenance critical parts, which are costly to repair

and replace, the starting forging stock received by the forging vendor and the forging preforms, used in forging production, are ultrasonically inspected. The final forging is sometimes ultrasonically inspected. *This last inspection can be avoided if the forging process is under good process control, because this inspection is usually a costly procedure.* The inspection surfaces must be ground to avoid ultrasonic noise and aid interpretation of the results.

The forging supplier prefers generally to *guarantee* that the forging will meet predetermined ultrasonic requirements when inspected after machining by the OEM or assemblers. After the forging is machined, it frequently endures a final ultrasonic inspection. Good process design and process control techniques can reduce the cost of inspection significantly. *A forging process that is in control theoretically does not have to be 100 percent inspected.*

Die Penetrant Inspection — Die penetrant inspection is used to detect discontinuities such as forging laps and cracks that are open to the surface of fully dense (nonporous) materials.

Structurally porous materials would give a false indication of a discontinuity. Again, the forging designer will add a forging allowance during the forging design process to facilitate using this inspection method. Another way to avoid the formation of discontinuities is to use process simulation for forging preform and die design, while making use of workability guidelines. A well designed forging preform distributes the material volume properly to assure proper die contact to prevent discontinuities from forming, while the workability guidelines, which is provided by the Dynamic Material Modeling (DMM) method, give the range of temperature and strain-rate where the material flow process and microstructure evolution is stable. Thus, good product and process

design procedures and knowledge about the requirements of inspection techniques can mitigate the need for expensive inspection procedures.

Magnetic Particle Inspection — Magnetic particle inspection is used to detect surface and near surface defects in ferromagnetic materials such as ferrous metal forgings. In this technique, an electric current is passed through the forging or induced with insulated electric coils. This application of current imposes a magnetic field on the forging. When the iron filings are distributed over the surface of the forging, surface and near surface defects are highlighted by adhesion of the iron filings about the localized break in the imposed magnetic field.

For simple shapes, magnetic particle inspection is cost effective in comparison to penetrant inspection. However, when complex netshape parts are inspected, magnetic particle inspection becomes so involved that the die penetrant method is usually more cost effective. Magnetic particle inspection is generally used only on forgings whose surfaces are not machined and the material is ferromagnetic. Most alloy steel forgings require complete machining to remove the decarburized layer, which is a loss of carbon from the surface of a steel forging by heating it above its lower critical temperature. The cost of magnetic particle inspection of such forgings would be wasted in this case, making die penetrant the preferred inspection method.

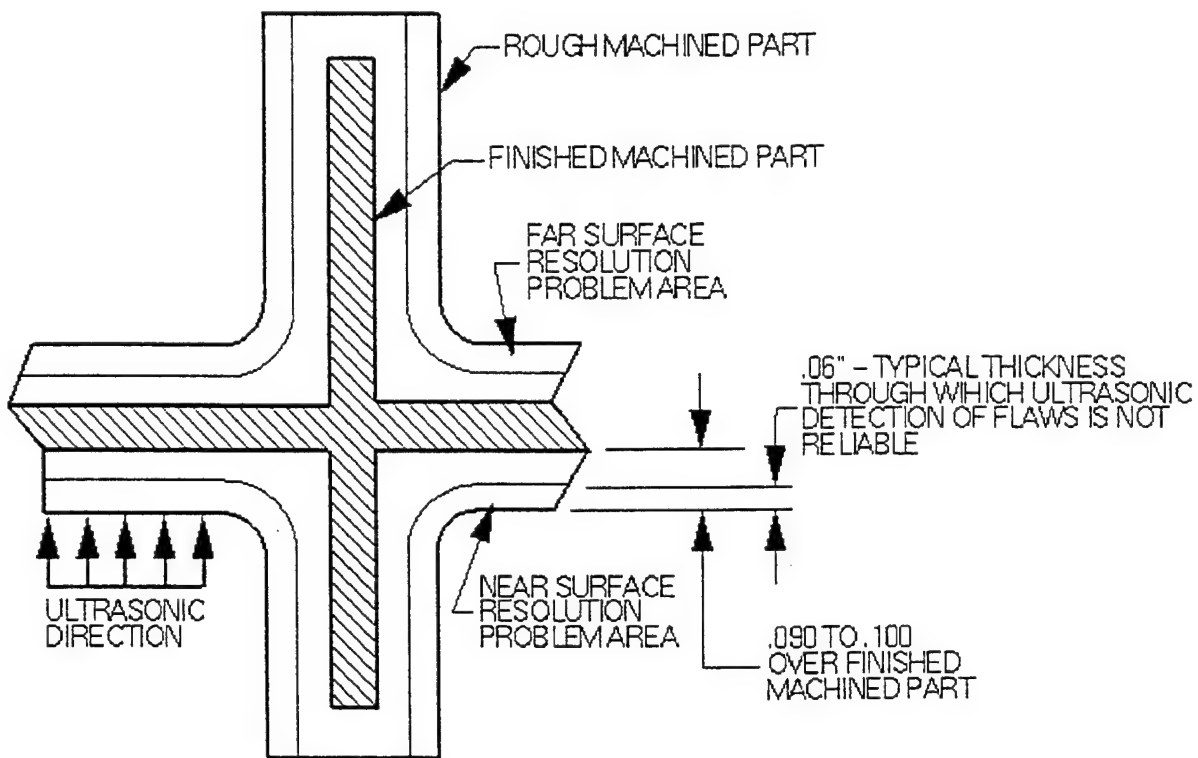


Figure 35. Ultrasonic Inspection, Near and Far Surface Resolution Problems

Precision or near Netshape forging requires the application of integrated engineering principles that produce complementary preform and die design solutions. The complete design must consider each independent process in the product realization chain, and this design should include the forging system, which consists of the *forge press*, the *control* system and the *material* system. The material system is defined to consist of the *workpiece*, the *die* materials, including *wear resisting coatings*, and the *lubricants*. Precision or near Netshape forging processes demand that the final forging dimensions be controlled at all times, making it necessary for the process designer to have a deep understanding of preform and die design practices and knowledge about the NDI inspection

methods that are used to control product quality. These relationships were discussed in the previous section.

Die Design also requires the designer to understand the relationships between the *process variables* and the *machine variables* and how these parameters interact to control the dimensions of the final forging, its microstructure and mechanical properties. This fundamental understanding is important, because one of the major goals of process design is to predict the product properties from known process variables. For example, the interactions of major process variables in hot deformation processes are illustrated in Figure 36. It is seen that the forging press used influences the process conditions. The flow stress, the interface friction, and the part geometry determine the forming load and energy. These process parameters, in turn, control the stress and strain factors in the tooling, and they ultimately determine the life of the forging die. The flow stress increases with increasing deformation rate and decreasing temperature. The magnitudes of these variations depend upon the specific workpiece material under consideration. The frictional conditions deteriorate with increasing die chilling.

The temperature departures during deformation, for a given initial workpiece temperature, are influenced mainly by the following process parameters:

Cause of Temperature Departures During Deformation

- The surface area of contact between the dies and the workpiece.
- The workpiece thickness and volume.
- The die temperature.

- The amount of heat generated by plastic deformation and friction.
- The contact time under pressure.

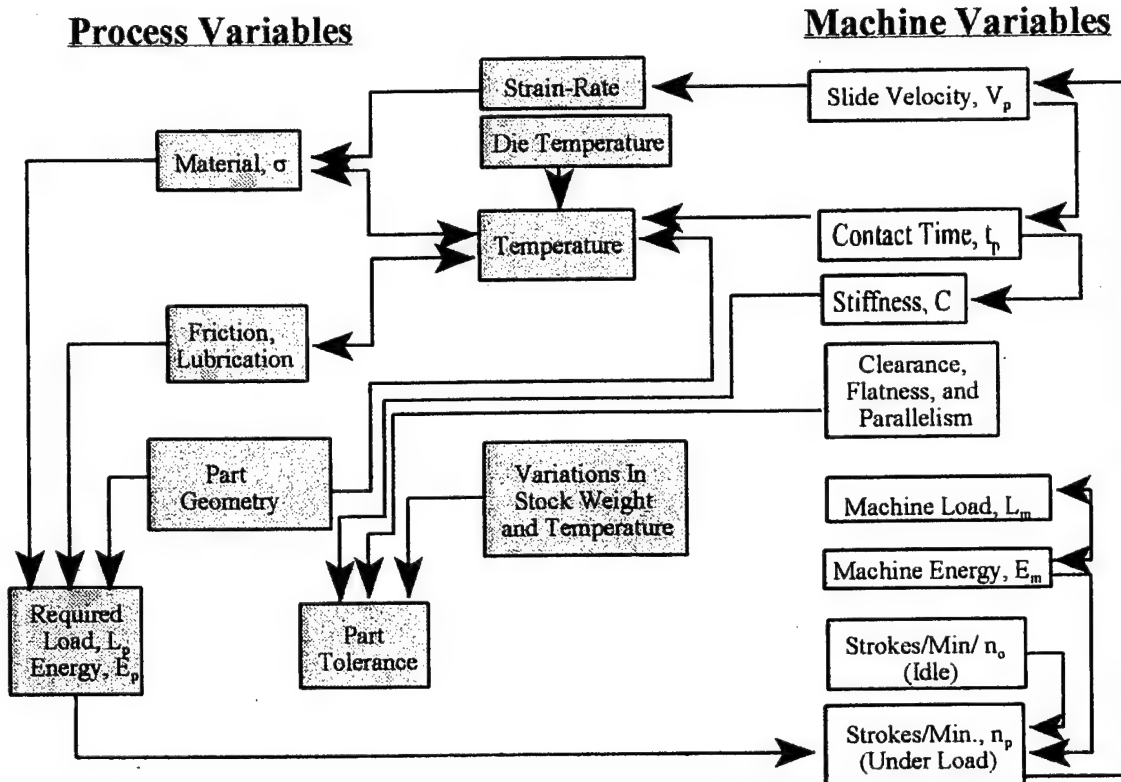


Figure 36. Relationships between Process Variables and Machine Variables

Part tolerance is controlled by three basic parameters shown in Figure 36, and they are as follows: the machine stiffness C , its clearance, flatness, and parallelism, and variations in forging stock weight and temperature. The type of die material, which is selected for making the dies, is controlled by the die temperature, the workpiece material flow properties, workpiece temperature, and the magnitude and type of load, such as static, impact, or repetitive loading.

In summary, die design for near Netshape forging involves determining the die stresses and strain factors, the elastic deflections of the individual die system components and stress trajectories through the forging die to the die support system. The workflow process for die design, shown in Figure 26, includes design activities for preform design, die stress analysis at the die impression, die bottom and at each interface of the die and die stack through to the press bolsters. Since near Netshape forging generally uses hot dies, predictions of die life and deformation by creep must be included in the analysis. The results of these analyses can be used subsequently for selecting the most appropriate die material.

4.4.3.1 Work Flow Process for Die Design

The Forging Design Sequence starts with a machine part drawing that is received from the part designer, who is usually an OEM Assembler or an Assembler. The objective is to design a finish forging shape, which includes all of the material allowances needed for dimensional control, microstructure/property achievement, and NDI inspection. Important process and die design activities are enumerated below:

Design clarification is the first step, and it is done to analyze the part drawing to identify basic geometrical features such as ribs, webs, and flanges to establish the relationships between the part features and the shape, which will form the machined die impressions.

Once designers understand the part design, they make drawings of the final forging shape. The drawings are similar to the one shown in Figure 28 with its applied forging allowances. This task is done to make certain that the forged shape meets dimensional requirements, for example, to machine undercuts and to assure those other forging areas, as appropriate, have tolerances to meet functional requirements. This drawing allows the designer to evaluate area and volume requirements along principal directions, which the datum planes define.

The forging-weight calculations of the as-forged shape are made to determine a starting weight by doing independently the following drawings: (a) The plan form area of the forging, (b) the forging outline plus saddle, and (c) the plan form area of forging plus saddle plus gutter.

Preform and blocker forge design is done to create the sequencing of necessary preforms for forging in closed die impressions to produce the preform for the finish forging. Area and volume distributions, at incremental die strokes and radial displacements of the developing preform shape, are done to identify centroids of component parts such as ribs, webs and flanges, matching areas and volumes with those of the finish shape.

Die designers adjust shape changes in the material preforming process to be compatible with the shape changes that occur in the finish shape. The objective of this design task is making certain that all necessary workability (strain limiting) criteria are satisfied and they produce

the desired microstructure in the newly finished shape. This data is used to develop admissible preform shapes that “streamline” the material flow to produce the final shape.

Converge the solutions of the preform shape by doing detailed analyses, which include the following:

- Analyses that define the material front displacements during the working stroke and each increment of the stroke along with the force to be exerted at each stage of deformation.
- Analyses that define each developing radius of curvature of the newly generated surfaces from the preform body as the workpiece flows into the die fillet radii, transition zones and deeper impression shapes.
- Analyses that evaluate the unsupported material front during working stroke with respect to fixed die boundaries.
- Analyses that determine the thickness of material fronts entering space provided by die contours for stability and support in each successive die.

Select the preform design that requires the least amount of energy to generate the finish shape. Complete this process by defining a sequence of shapes starting with the initial billet and ending with the preform shape that produces the new finish forging. Principal and equivalent strains should be calculated for each intermediate shape and the finish shape.

Detail die design as shown in Figure 15 is the next stage. The next important die design task is to *calculate the force* required to make final forging shape. The force and energy required in the finish operation is calculated for each stage of die filling. These calculations are based on material and die temperatures, strain-rate and strain level, and the input preform shape that is determined by the shape sequencing analysis. In this analysis, the force required to make the final forging shape is determined in stages. These disparate force calculations are as follows: (a) Fill Die Cavity, (b) Create Saddle Width Beyond Forging, (c) Partially Fill the Flash Gutter, (d) Close Dies for Die Bearing Surface Contact and Force Transmitted Through Die and Press Supports.

Equilibrium elasticity analyses are made to determine elastic die deflections. At this stage the designer can compare the elastic deflections of alternative die materials. A spread sheet for a complete design interaction approach is generally done, where the interaction approach is to vary sizes, strain levels, and forces to specify the die diameter and thickness compatible with the die support system.

Next, the die designer does a separate analysis of the *strain concentration factors*. This analysis is done within the die impression and on the die outer shapes, such as ejector holes, locks, thermocouple holes, and threaded surfaces. For example, elasticity analysis of the dies determines the dimensions of the saddle area. If the die loading during the forging process is cyclical, the designer should do a stress factor calculation to include the effect of fatigue on die life. A wear analysis can be done to show the areas that will be prone to wear by abrasion, and candidate surface regions for surface hardening by ion implantation or chemical vapor deposition (CVD).

Die drawings are prepared as required based on the detailed results of simulation-based design. This activity includes any open draw dies, preform dies and finish dies or inserts, including impressions, bearing and cleared surfaces, locking and attaching methods, ejection designs and thermocouple holes.

4.4.3.2 Stress and Strain Concentration Factors

Strength of Material theories are used in the design of die systems relate uniaxial, biaxial and triaxial stress systems. Elastic analysis of the dies is done to make certain enough die material exists to distribute the load satisfactorily. Designers usually base the calculated load carrying capacities of dies on nominal stresses. Designers handle the concentrations of strain and stress caused by fillets, grooves, holes or other changes in section geometry separately. The local shape change produces effects that are confined to the specified zone.

Elastic stress analysis is done in these local zones, because discontinuities in the die shape affect the load only at the local region. These local zones are the ones where failure is likely to occur. Thus, separate analyses are required for particular shapes.

Strength Theories Used in Die Systems — The strength theories, which are generally used to design die systems, relate different states of stress. They are used for “brittle” materials, where the tensile elongations are < 5%. The *Normal Stress Criterion* and the *Mohr Circle theory* are used commonly. The *Normal Stress* theory asserts that failure occurs in a multiaxial system when either a *principal stress reaches the uniaxial tensile strength*, or a *principal compressive stress reaches the uniaxial compressive strength*. Thus,

$$\sigma_1 = \sigma_{UTS} \quad \sigma_3 = \sigma_{comp}, \text{ and } \sigma_1 > \sigma_2 > \sigma_3. \quad (35)$$

The Mohr Circle theory establishes circles of diameters equal to the *compressive ultimate tensile strength* and *tensile ultimate tensile strength*, and a constructed tangent line defines the condition of failure. Mohr's Circle Diagram is constructed from the following equations:

$$\sigma = \sigma_{\max} \cos^2 \alpha + \sigma_{\min} \sin^2 \alpha \quad (36)$$

$$\sigma = \frac{\sigma_{\max} + \sigma_{\min}}{2} + \frac{\sigma_{\max} - \sigma_{\min}}{2} \cos 2\alpha \quad (37)$$

$$\tau = \frac{\sigma_{\min} - \sigma_{\max}}{2} \sin 2\alpha \quad (38)$$

$$d = \frac{\sigma_{\max} - \sigma_{\min}}{2} \text{ and } r = \frac{\sigma_{\max} - \sigma_{\min}}{2} \quad (39)$$

The following equation can express a circle of a diameter and a radius:

$$(\sigma - d)^2 + \tau^2 = r^2 \quad (40)$$

The *Maximum Shear Stress* theory asserts that failure occurs when the maximum shear stress $\frac{(\sigma_1 - \sigma_3)}{2}$ in a multiaxial stress system reaches the value of the shear stress in a uniaxial tensile bar at failure. The following equation expresses this criterion:

$$\frac{\sigma_1 - \sigma_3}{2} = \frac{\sigma_f}{2} \quad (41)$$

Notch Sensitivity Equations — Beyond the application of these elementary strength theories, considerations of notch sensitivities such as K_t for steady stress, K_f for alternating stress and $\eta_k = \frac{k_f - 1}{k_t - 1}$ for combined steady plus alternating stress. Where, K_t is the theoretical (purely elastic) stress concentration factor, K_f is the ratio of unnotched fatigue strength to the notched

fatigue strength, and η_k is the material notch sensitivity. Frequently, designers call K_t the *stress concentration factor* or the *strain concentration factor* interchangeably. We give the theoretical definition of K_t as follows:

$$K_t = \frac{\sigma_{\max}}{\sigma_{\text{nominal}}} = \frac{\varepsilon_{\max}}{\varepsilon_{\text{nominal}}} \quad (42)$$

The K_t refers to the ultimate (maximum) value and σ_{nominal} is the failure stress based on the net section. σ_{\max} is a conceptual value, which is impossible to measure by direct methods, because it refers to a mathematical point on the net section at the end of a notch. The method of notch-strength analysis is based on the following assumptions:

- One must modify K_t to adapt to the size effect for every material.
- Designers must adapt the stress concentration factor to account for ductility, except materials that are strictly elastic such as glass and ceramics.
- Failure will take place for a critical value of σ_{\max} .

For the limiting case of cracks where the radius $\rho \rightarrow$ zero and $\sigma_{\text{nominal}} < \sigma_{\text{UTS}}$, the stress concentration takes the $K_t = 1 + C \sqrt{\frac{a}{\rho}}$ form, where a being the half width of an elliptical crack, and the nominal stress is given as $\sigma_{\text{nominal}} = \frac{\sigma_{\text{UTS}}}{K_t}$. A practical application of this mathematical form for K_t is to calculate the stress concentration factor for a die with a given *impression depth* and a *fillet radius*. The practical expression for K_t is as follows:

$$K_t = 1.0 + 0.50 \left(\frac{\text{depth of impression}}{\text{die fillet radius}} \right)^{\frac{1}{2}} \quad (43)$$

Table IV shows how the K_t varies as a function if *die fillet radii* for a constant *depth of impression*, which is equal to 2.0 inches.

Table IV. Calculated Stress Concentration Factors		
Stress Concentration Factor K_t	Die Fillet Radius (inch)	Remarks
3.04	0.12	Experience suggests that when K_t is > 2.0 the die designer should consider using a die insert rather than a monolithic die to avoid a catastrophic failure of the die by fracture.
2.41	0.25	
2.15	0.38	
2.0	0.50	
1.50	1.00	

A theoretical basis for the K_t to equal 2.0 as a limiting case for die stability is derived. By considering two special cases of *Stresses Around a Cylindrical Cavity*, one can show that K_t has a limiting value of 2.0 for an elastic material that has limited ductility whose stress follows a power law relationship such as $\sigma = \sigma_0 \dot{\epsilon}^m$ in high temperature deformation (creep), where, m is the strain-rate sensitivity factor of the material.

Stress Concentration in a Heavy Walled Cylinder under Internal Pressure — One can obtain an expression for K_t using a constitutive equation that models the strain hardening behavior of a material. One such constitutive equation has the following form:

Where, $(\sigma_o, \bar{\epsilon}_o, n)$ are constants. The K_t can be computed for the case of a circular hole with a radius $r = r_1$ as the ratio of the circumferential tensile stress σ_t at the hole $r = r_1$ to the stress σ at $r = \infty$ such that

$$\bar{\sigma} = \sigma_o \left(\frac{\bar{\epsilon}}{\bar{\epsilon}_o} \right)^n \quad 0 \leq n \leq 1 \quad (44)$$

$$K_t = \frac{(\sigma_t)_{r=r_1}}{\sigma} = \left(\frac{2}{1 + 3n} \right)^{\frac{2n}{(1 - 3n)}} \quad (45)$$

The factor K_t is a function of exponent n of the power law, and it is nearly approximated by

$$K_t = 1 + n, \quad (0 \leq n \leq 1) \quad (46)$$

If n is taken equal to zero, the stress concentration factor K_t becomes equal to unity, which is the case of an ideally plastic material. When the exponent n is chosen equal to unity, a second limiting case is obtained, and a stress concentration factor $K_t = 2$. *This second limiting case of the power function law coincides with the law of elasticity for incompressible materials.*

However, when n is equal to $\frac{1}{3}$ the stress concentration factor becomes indefinite, but if

$\alpha = \frac{2n}{(1 - 3n)}$ such that when $n = \frac{1}{3}$, $\alpha = \infty$, K_t appears in the form:

$$K_t = \frac{\lim}{\alpha \rightarrow \infty} \left(1 + \frac{1}{3\alpha} \right)^\alpha, \quad (47)$$

which is equal to $e^{\frac{1}{3}} = 1.396$. Therefore, a disk that yields under a strain hardening law has a strain concentration factor that varies in the range $1 \leq K_t \leq 2$, and this corresponds to the two limiting cases of ideally plastic and the perfectly elastic substances, respectively.

Die materials behave almost like a perfectly elastic substance when their total elongations do not exceed 5% in tension, and most die materials do not. *Therefore, the empirical criterion that a die designer should consider using die inserts when the stress concentration factor K_t exceeds two is a reasonable rule based on theoretical considerations.*

Creep of a Hollow Cylindrical Cavity — If the die cavity contains a cylindrical cavity of radius $r = r_1$, one finds for the steady state stage of creep following this power function velocity law that

$$\sigma_t = \sigma \left[1 + (2m - 1) \left(\frac{r_1}{r} \right)^{2m} \right] \quad (48)$$

the radial and tangential stresses are given by the following formulas:

$$\sigma_r = \sigma \left[1 - \left(\frac{r}{r_1} \right)^{2m} \right], \quad (49)$$

Around the surface of the cylindrical cavity, the tangential stress is equal to $r = r_1$, $\sigma_t = 2m\sigma$, and the stress concentration factor $K_t = 2m$. This factor will be greater than unity as long as the exponent m of the power velocity function is $.5 < m < 1$, and that a stress concentration factor under *steady state creep* occurs measured by the factor $K_t = 2m$ under these circumstances. In an elastic body, upon applying the stress σ , $K_t = 2$, but, after the redistribution of stress by creep, the stress concentration factor K_t is reduced to $2m$ smaller than 2, except in the case when $m = 1$, in a purely viscous substance, when $K_t = 2$ remains unchanged.

Each of the strength theories that are applied to a particular component uses *average* stress values. In contrast, the relationships used in design are based on structures having a constant cross-section with gradually changing contours. The calculated nominal stress is modified by a strain concentration factor that accounts for abrupt changes in geometry. This phenomenon is characteristic of elastic behavior. Plastic yielding accompanies high stresses, which tends to mitigate strain concentrations, and this behavior is true in relatively brittle materials. The localization of stresses also depends on whether the material is ductile or brittle.

Cross-sectional shape change results in changing the distribution of stresses, depending on the magnitude and the type of load. The various types of loads are as follows:

- Static
- Impact
- Repetitive
- Concentrated
- Uniform
- Creep

The die designer must select the appropriate stress or strain concentration factor depending on whether the material exhibits elastic behavior and the type of loading. The rules for die design are based on having a practical knowledge of how a particular value of stress or strain concentration factor should be correlated to the choice of die design. For example, the decision to use a die insert design versus a monolithic die design depends on the value of the stress or strain concentration factor.

4.5 SHAPE OPTIMIZATION

4.5.1 Introduction

The preceding section emphasized the importance of controlling the dimensions of precision or net shape forgings, and the reasons for controlling are listed in section 4.4.2.1. Forging allowances are added to the basic machine-part geometry to produce a forging envelop. Datum planes are

established in the principal length and width directions in an attempt to control the weight of forgings by dividing the masses into two equal parts. The next important step in designing the forging process is to find by some method a preform shape. *One rule that experienced die designers use in discovering a preform shape is that the preform shape should fill the impression zone of the finish die with the least amount of energy. A corollary to this rule is that the ideal preform shape is one that also fills the finish die with the least amount of metal flow.* The process of "streamlining" distributes metal from a primitive shape such as a cylinder or a block to some final shape having distinctive geometrical features. Streamlining requires the process designer to have a fundamental knowledge about how geometry influences the metal flow direction. The process designer must also understand the intrinsic workability of the workpiece material and how it constrains the temperature and strain-rate process parameters. The concept of "limiting strains" must be understood in the framework or context of intrinsic workability.

A forging designer usually has a practical understanding of limiting strains, and, in this context, the forging engineer must distinguish the difference in meaning of limiting strain with respect to cold forming and hot working. In cold forming, the limiting strain, as expressed by some criterion such as the Cockcroft and Latham¹ fracture criterion, where the strains at fracture correlates with this criterion. During hot working, the concept of limit strain is different. *In this case, the forging engineer is concerned with a minimum-strain that represents a condition for which the workpiece material has undergone this minimum-strain throughout the entire volume.* This minimum strain,

¹H.A. Kuhn, P.W. Lee, and T. Erturk: *J. Eng. Mat. Technol., Trans. ASME*, 1973, 95H, p. 213.

in effect, represents the time that is necessary for the workpiece to go through a number of dissipated energy states and intermediate microstructures until a stable microstructure is reached. This stable microstructure will correspond to a steady state condition during which time the microstructure sensitive properties such as Fracture Toughness K_{IC} and Low Cycle Fatigue (LCF) do not change with continued deformation (strain). In fact, this is the reason that simple compression tests can be used to simulate the plastic flow behavior of engineering alloys at strain levels that far exceed the strain levels, which are attainable, in a well lubricated compression test. *All that is required of the compression test is that the flow stress of the material approach steady state asymptotically.*

The forging engineer and die designer have a need for a rapid technique that will reveal to them admissible intermediate states as they are influenced by the finish forging geometry. The number of intermediate states will be determined by the intrinsic workability of the workpiece material, the lubricant characteristics and the thermal and mechanical properties of the die material, which include wear resistance, hot tensile strength, fracture toughness, low cycle fatigue and thermal fatigue properties.

The development of an intelligent optimization-based design system is a necessity for minimizing the amount of trial and error done on the shop floor. The goal is to be able to optimize the metal forming process off-line such that the process design engineer can focus the design effort to finding optimal solutions. Exploratory research was done to develop a methodology for doing preform design by geometrical mapping material trajectories during forging.

The designer starts with the final desired shape and a sequence of preforms are designed such that the primary cylindrical billet shape is transformed into the final shape in a series of forge steps. The design of preforms, once available, can be evaluated using established finite element techniques to validate their validity. The results obtained from simulation display the forge behavior with high accuracy, and the data is utilized to change the design in its geometric proximity to correct any problems that may exist. Such *post facto* evaluation results in designs that work, but not necessarily designs that are optimal. The principal difficulty in developing optimal designs lies in the lack of *a priori* knowledge of the backward map from the final shape to the initial shape. As a result, the design process relies heavily on experience and judgement.

The ideal aim is to find material deformation trajectories, which not only change from the billet to the final geometry, but also deform the material in its favorable processing window, i.e., in the strain, strain-rate and temperature space. Thus, the optimal material trajectory determination satisfies simultaneously both the stable flow requirements for the material and an efficient deformation sequence.

The primary goal behind geometric mapping of material trajectories during forging is to facilitate shape optimization. Shape optimization is done by taking a global view of the material deformation streaklines (point trajectories) during the forging operation and to perform *a priori* adjustments in the process to maximize the material performance (workability). The basic premise behind this approach is that optimization must be performed with a global perspective rather than only at individual time points during the progression of the manufacturing operation. This means that the

optimal trajectory could entail material deformation in a non optimal manner in the beginning so that the flow at a later stage is easier and vice versa. The trajectory optimization procedure starts with the geometric mapping and optimal control techniques. The objective is to minimize a cost function, which includes quadratic terms. These terms express the loss of performance caused by deviation from a prescribed path. The geometric mapping is developed such that it allows for construction of a cost function in terms of the states of the forge system, which is minimized.

The trajectory-based shape optimization, which builds upon the geometric mapping techniques, is intended for effective use in developing new process designs. This method fills the important void of mapping of the initial shape to the desired final shape, which cannot be *a priori* performed using numerical techniques such as the finite element method (FEM). The trajectory optimization is intended to develop optimal designs based on simplified methods, which may then be verified using the FEM. Such a design, when completed, is thought to have a substantial potential of being close to the true optimal design as defined by the user-specific cost function.

The trajectory optimization needs material velocity at the boundary and internal points of interest as the state variables. The strain evolution in the material is then determined using the spatial gradient of velocity. The objective is to develop the desired strain pattern in the forge shape while ensuring that the material stays within a desirable processing window. The state variables are altered using admissible control inputs during the forge process. These inputs comprise incompressible velocity fields, which obey the basic shape related symmetry boundary conditions, and they are generated using the divergence free functions, which obey radiation and finiteness conditions. These

admissible fields are to be used for superimposition upon the trial (non optimal) mapping of shape from the initial to final geometry to allow perturbation of the mapping in an admissible fashion. This perturbed mapping is then evaluated using a user-defined cost function to obtain an optimal solution.

The present report explains the two methods that were studied with the objective of forge process optimization as follows:

A FEM-based multi variable optimization of forging: This is explained in Section 3.5.3.

The major accomplishment of this effort was to develop processing conditions for a gamma TiAl alloy automotive valve preform forging. This approach was based upon posing the trajectory optimization as a multi variable optimization solution, while developing the cost function entries based upon FEM solutions. Even though the objective of forge process optimization was accomplished, an important difficulty in this approach surfaced. The time expended in performing the FEM solution was too long.

Geometrical Mapping Procedure: The geometric mapping procedure for determination of material streaklines. The output of this effort is the starting point for trajectory optimization of the forging process. The geometric mapping procedure is based upon utilization of divergence free Green's functions. They provide the necessary external control to facilitate optimization calculations.

The governing equations for the forging process, which are common to every solution approach, are presented in Section 4.5.2.

4.5.2 Governing Equations for Material Flow

The material flow in the forging process can be viewed as Stoke's flow. The material is considered to be incompressible. The governing equations are given as follows:

An admissible velocity field, v , needs to satisfy the continuity equation, which states that the divergence of the velocity field is zero. Or,

$$\nabla \cdot V = 0 \quad (50)$$

The equilibrium equation is given by:

$$-\frac{\nabla p}{\rho} + \nu \nabla^2 V = 0 \quad (51)$$

The material constitutive law is given by:

$$\sigma = f(\varepsilon, \dot{\varepsilon}, T) \quad (52)$$

where σ is the flow stress, which is a function of strain, strain-rate and temperature.

These equations are solved along with the time evolving Dirichlet, Neumann and Mixed boundary conditions² to predict the material flow during the forging process.

² The problem of finding a solution, which takes on given boundary values is known as a *Dirichlet problem in honor of P. G. I. Dirichlet (1805-1859)*. In contrast, if the values of the normal derivative are prescribed on the boundary, the problem is said to be a *Neumann problem in honor of Karl Gotfried Neumann (1832-1925)*. Dirichlet's and Neumann's problems are also known as the first and second boundary value problems of potential theory, including velocity (stream) potential, perfectly elastic torsion (warping function).

5.0 CONCLUSIONS

The objective of this Phase II SBIR Project was to develop simulation-based process design methodologies and tools for intelligently optimizing and controlling metal forming processes. Emphasis was placed on understanding the evolution of microstructure and the relationships between constitutive relationships (flow stress), the dynamic material model (intrinsic workability) and microstructure development during hot deformation. The research and development approach was based on fundamental concepts that have emerged from control theory and dynamic material modeling. These concepts were used to develop an optimization-based design approach for shape and microstructure optimization.

A new process design method for controlling microstructure development for precision forging was developed. The challenge of effectively controlling the values and distribution of important microstructural features can now be systematically formulated and solved in terms of an optimal control problem. This method was applied to the optimization of grain size and certain process parameters such as die geometry profile and ram velocity during extrusion of plain carbon steel. Various case studies were investigated, and experimental results showed good agreement with those predicted in the design stage. A software product for *Microstructure Trajectory Optimization* was developed, and it is now ready for beta site testing.

Modeling and simulation of metal forming equipment was done to better understand and improve

the control of metal forming equipment. Techniques were developed for creating accurate models and computer simulations of metal forming equipment. These principles were applied to modeling and simulation of the 1000 ton forge press in service in the Experimental Material Processing Laboratory (EMPL), Wright-Patterson AFB Ohio. Physical modeling was done also to verify the modeling methodology. These EMPL results indicate that considerable opportunity exists for increasing the life of servohydraulic systems and reducing the cost of maintenance. It was also shown that the press model can be integrated into the ANTAREST™ FEA application. This capability allows the process designer to run the forging simulation as a virtual process, making the results very realistic.

A workflow process for precision die design was developed to understand more precisely how optimization-based preform design can be used to improve die design and reduce the cycle time. The controlling driver in manufacturing is cost reduction for all forged components used to fabricate structures. The focus on forged component manufacturing cost reduction through realistic process design will contribute significantly to the reduction of acquisition costs for new products. This task addressed the aggressive goal for cost reduction and brings focus to the relative processing requirements and cost performance of candidate high strength aerospace and automotive product forms used by OEM's, subcontractors and machining sources in the component manufacturing streams.

A Metallurgists' Notepad software application was developed. This software application allows materials specialists and process engineers to acquire process design data for remote databases using the capabilities offered by the World Wide Web (WWW). The possibility of future implementation of the Metallurgists' Notepad as a fully browser-based intranet application was studied. This study investigated such issues as incorporating the following (a) Java, C, and ActiveX, (b) Internet Relay Chat (IRC), (c) ODBC database, and (d) multi-media elements.

Some additional areas of concern included the following: (a) Computations of Dynamic Material Model Stability Criteria, (b) Database Access, (c) User Training, (d) User Interface, (e) the Development Environment, and (f) Security. Analysis was done to develop a more generalized database structure to support the full range of data retrieval, analysis, export, and reports. A new materials property software application has resulted from this work and will be made available as a commercial product.

6.0 COMMERCIALIZATION

UES Software has implemented a product development plan that will incorporate the most mature and tested modules in a new ANTAREST™ version. This version will have a new interface, which will be available on PC Windows NT and UNIX workstations.

7.0 REFERENCES

1. Kirk, D. E., 1970, *Optimal Control Theory: An Introduction*, Prentice-Hall.
2. Jonas, J.J., Sellars, C.M., and McG, Tegart, 1969, Strength and Structure under Hot Working, *Metall. Rev.*, Vol. 14 (No. 1).
3. Sellars, C.M., 1978, Recrystallization of Metals During Hot Deformation, *Philos. Trans. Roy. Soc.*, Vol. 288 (No. 147).
4. McQueen, H.J. and Jonas, J.J., 1975, Recovery and Recrystallization During High Temperature Deformation, in *Treatise on Materials Science and Technology*, Vol. 6, *Plastic Deformation of Materials*, Academic Press, pp.393-493.
5. Roberts, W., 1984, Dynamic Changes That Occur During Hot Working and Their Significance Regarding Microstructural Development and Hot Workability, in *Deformation, Processing, and Structure*, G. Krauss, Ed., ASM International, pp.109-184.
6. Malas, J.C., 1991, "Methodology for Design and Control of Thermomechanical Processes," Ph.D. dissertation, Ohio University.
7. Malas, J.C. and Seetharaman, V., 1992, Use of Material Behavior Models in the Development of Process Control Strategies, *JOM*, Vol. 44 (No. 6).
8. Frost, H.J., and Ashby, M.F., 1982, *Deformation Maps*, Pergamon Press.
9. Raj, R., 1981, Development of a Processing Map for Use in Warm-Forming and Hot-Forming Process, *Metall. Trans. A*, Vol. 12, p. 1089.

10. Frazier, W. G., 1995, "Robust Control Techniques for Hot Deformation Processes", Contributive Research and Development, Volume 228, SYSTRAN Corp. Final Report, Task 178, Contract F33615-90-C-5944, March.
11. Kumar, A., Rao, K.P., Hawbolt, E.B., and Samarasekera, I.V., 1987, The Application of Constitutive Equations for Use in the Finite Element Analysis of Hot Rolling Steel, Unpublished Research.
12. Devadas, C., Samarasekera, I.V., and Hawbolt, E.B., 1991, The Thermal and Metallurgical State of Steel Strip during Hot Rolling: Part III. Microstructural Evolution, *Metall. Trans. A*, Vol. 22A., pp. 335-349.
13. Yada, H., 1987, Prediction of Microstructural Changes and Mechanical Properties in Hot Strip Rolling, *Proc. Int. Symp. Accelerated Cooling of Rolled Steels*, Conf. of Metallurgists, CIM, Winnipeg, MB, Canada, Aug. 24-26, G.E. Ruddle and A.F. Crawley, Eds., Pergamon Press, Canada, pp. 105-20.
14. Senuma, T. and Yada, H., 1986, Annealing Processes, Recovery, Recrystallization and Grain Growth, *Proc. 7th Riso Int. Symp. on Metallurgy and Materials science*, Sept. 8-12. Suehiro, M., Sato, K., Tsukano, Y., Yada, H., Senuma, T. and Matsumura, Y., 1987, *Trans. Iron Steel Inst. Japan*, Vol. 27, pp. 439-45.
15. Srinivasan, R., Gunasekera, J.S., Gegel, H.L, and Doraivelu, S.M., 1990, Extrusion Through Controlled Strain-rate Dies, *J. Material Shaping Technology*, Vol. 8, No. 2, pp. 133-141.
16. Vander Voort, 1984, in *Metallography, Principles and Practice*, McGraw Hill Book Co., New York, p. 410.

17. UES, Inc., 1995, *Antares Software User Manual*.
18. Wayne Anderson (1988), Controlling Electrohydraulic Systems, Marcel Dekker, New York.
19. Ernest E. Lewis and Hansjoerg Stern (1962), Design of Hydraulic Control Systems, McGraw-Hill, New York
20. Duone Tandeske (1991), Pressure Sensors, Marcel Dekker, New York.
21. Harry N. Norton (1969), Handbook of Transducers for Electronic Measuring Systems, Prentice-Hall, Englewood Cliffs, New Jersey.
22. Paul M. DeRusso, Rob J. Roy, and Charles M. Close (1965), State-Variables for Engineers, John Wiley and Sons, New York.
23. S. Bennet and D.A. Linkens (1982), Computer Control of Industrial Processes, Peter Peregrinus, LTD, New York
24. John G. Truxal (1955), Control System Synthesis, McGraw-Hill, New York.
25. Law and W. D. Kelton (1991), Simulation Modeling and Analysis, McGraw-Hill, Inc., New York, 2nd Edition, pp. 1-6, 109-116.

References 1 through 17 refer to Section 4.2. References 17 through 25 refer to Section 4.3.

Reference 17 of Section 4.2 is equivalent to reference 1 of Section 4.3.